Heterodinuclear Catalysts Zn(II)/M and Mg(II)/M, Where M = Na(I), Ca(II) or Cd(II), for Phthalic Anhydride/Cyclohexene Oxide Ring Opening Copolymerisation

Arron C. Deacy,[a] Christopher B. Durr ,[a] Ryan W. F. Kerr[a] and Charlotte K. Williams[a]*

[a]Department of Chemistry, Chemistry Research Laboratory, 12 Mansfield Rd, Oxford, OX1 3TA. *Charlotte.williams@chem.ox.ac.uk.

Experimental Section

All experiments were performed using a dual-manifold nitrogen-vacuum Schlenk line or in a nitrogen filled glovebox. All solvents and reagents were obtained from commercial sources and used as received unless stated otherwise. THF and pentane were dried using a SPS system and de-gassed by several freeze-pump-thaw cycles, before being stored over activated 3 Å molecular sieves under nitrogen. Cyclohexene oxide was dried over calcium hydride for 48 hours and purified by fractional distillation and stored under nitrogen. Phthalic anhydride was purified extraction into benzene, followed by crystallization from chloroform and the final product was sublimed. All deuterated solvents were dried over calcium hydride for 16 hours and purified via vacuum transfer.
Gel permeation chromatography (GPC) analyses were carried out using a Shimadzu LC-20AD instrument, at 40 °C, with two mixed bed PSS SDV linear S columns in series and THF at a flow rate of 1 mL min^{-1}. Polymer molecular masses (M_n) were obtained by calibration of the instrument using a series of narrow molecular mass polystyrene standards. Elemental analyses were conducted by Mr. Stephen Boyer at London Metropolitan University.

Complex 1: $Li(N(SiMe_3)_2)$ (0.27 g, 1.62 mmol) was added to a solution of H_2L (0.30 g, 0.81 mmol), in THF (5 mL), at 25 °C, and a colour change from yellow to colourless was observed. The solvent was reduced, in *vacuo*, to dryness, and the crude product was washed with pentane to afford a white solid (0.29 g, 0.77 mmol, 95 %). ^{1}H NMR (d_8-THF, 400.20 MHz, 298 K) 7.89 (s, 2H, **H**C=N) 6.65 (d, ^3J = 7.83 Hz, 2H, *o*-Ph**H**) 6.54 (d, ^3J = 7.48, 2H, *m*-Ph**H**) 6.18 (t, ^3J = 7.83 Hz, 2H, *p*-Ph**H**) 3.65 (s, 6H, -OC**H**$_3$) 3.15 (s, 4H, N-C**H**$_2$-) 0.65 (s, 6H, -C(C**H**$_3$)$_2$). ^{7}Li NMR (d_8-THF, 155.52 MHz, 298 K) 1.44 ppm. ^{13}C{^{1}H} NMR (d_8-THF, 125.81 MHz, 298 K) 164.5 (H**C**=N) 160.8 (ipso-**Ph**) 152.9 (*o*-**Ph**-OCH$_3$) 126.2 (*m*-**Ph**-CH=N) 122.5 (*o*-**Ph**-CH=N) 110.9 (*p*-**Ph**) 110.3 (*m*-**Ph**-OCH$_3$) 75.5 (N-**C**H$_2$-C(CH$_3$)$_2$) 55.4 (-O**C**H$_3$) 36.6 (-**C**(CH$_3$)$_2$) 23.0 (-C(**C**H$_3$)$_2$). Elemental Analysis for $C_{21}H_{24}Li_2N_2O_4$ (382.21 $gmol^{-1}$): Calculated; C, 66.0; H, 6.3; N, 7.3 %. Found: C, 65.9; H, 6.4; N, 7.3 %.

Complex 2: $LiN(SiMe_3)_2$ (0.23 g, 1.35 mmol) was added to a solution of H_2L (0.25 g, 0.68 mmol) in THF (5 mL). A solution of ZnI_2 (0.48 g, 2.70 mmol) was added and a pale yellow precipitate was formed. The solute was decanted and the solid was washed with THF, then pentane and dried in *vacuo* to afford a pale yellow solid (0.41 g, 0.54 mmol, 80 %). ^{1}H NMR (d_8-THF, 400.20 MHz, 298 K) 7.97 (s, 2H, **H**C=N) 6.76 (d, ^{3}J = 7.83 Hz, ^{4}J = 1.49 Hz, 2H, *o*-Ph**H**) 6.67 (d, ^{3}J = 7.83, ^{4}J = 1.23 Hz, 2H, *m*-Ph**H**) 6.30 (t, ^{3}J = 8.09 Hz, 2H, *p*-Ph**H**) 4.63 (br. m, 2H, -C**H**$_2$) 3.89 (s, 6H, -OC**H**$_3$) 2.95 (br. m, 2H, -C**H**$_2$) 1.03 (s, 3H, -C**H**$_3$) 0.67 (br. s, 3H, -C**H**$_3$). ^{13}C{^{1}H} NMR (d_8-THF, 125.81 MHz, 298 K) 168.2 (H**C**=N) 160.7 (*ipso*-**Ph**) 151.7 (*o*-**Ph**-OCH$_3$) 126.8 (*m*-**Ph**-CH=N) 118.7 (*o*-**Ph**-CH=N) 112.1 (*p*-**Ph**) 111.9 (*m*-**Ph**-OCH$_3$) 73.9 (N-**C**H$_2$-C(CH$_3$)$_2$) 55. 4 (-O**C**H$_3$) 36.5 (-**C**(CH$_3$)$_2$) 26.2 (-C(**C**H$_3$)$_2$). Elemental Analysis for $C_{21}H_{24}I_2N_2O_4Zn_2$ (749.84 $gmol^{-1}$): Calculated; C, 33.5; H, 3.2; N, 3.7 %. Found: C, 33.3; H, 3.3; N, 3.6 %.

Complex 3: $ZnEt_2$ (0.17 g, 1.35 mmol) was added dropwise to a solution of H_2L (0.5 g, 1.35 mmol), in THF (10 mL), and the solution was stirred at 25 °C for 16 h by which time a pale yellow precipitate formed. The solution was filtered and the solid washed with pentane (3 x 5 mL) and dried *in vacuo* to afford the product as a pale yellow solid (0.44 g, 1.01 mmol, 75 %). ^{1}H NMR (400.20 MHz, $CDCl_3$, 298 K) 7.87 (s, 2H, **H**C=N), 6.80 (dd, ^{3}J = 7.44 Hz, ^{4}J = 1.56 Hz, 2H, Ph**H**) 6.67 (dd, ^{3}J = 7.96 Hz, ^{4}J = 1.41 Hz, 2H, Ph**H**), 6.45 (t, ^{3}J = 7.74, 2H, Ph**H**), 3.75 (s, 6H, -OC**H**$_3$), 3.41 (Br., 4H, N-C**H**$_2$-C(CH$_3$)$_2$) 0.88 (s, 6H, -C(C**H**$_3$)$_2$). ^{13}C{^{1}H} NMR (125.81 MHz, $CDCl_3$, 298 K) 168.6 (H**C**=N) 161.2 (*ipso*-**Ph**) 152.5 (*o*-**Ph**-OCH$_3$) 126.8 (*m*-**Ph**-CH=N) 120.0 (*o*-**Ph**-CH=N) 117.1 (p-**Ph**) 113.5 (*m*-**Ph**) 73.1 (N-**C**H$_2$-C(CH$_3$)$_2$) 56.9 (-O**C**H$_3$) 36.1 (-**C**(CH$_3$)$_2$) 25.3 (-C(**C**H$_3$)$_2$). Elemental Analysis for $C_{21}H_{24}N_2O_4Zn$ (432.10 $gmol^{-1}$): Calculated; C, 58.1; H, 5.6; N, 6.5 %. Found; C, 57.9; H, 5.7; N, 6.4 %.

Complex 4: $ZnEt_2$ (0.07 g, 0.54 mmol) was added dropwise to a solution of H_2L (0.20 g, 0.54 mmol), in THF (5 mL), and the solution was stirred at 25 °C for 4 h. Next, NaI (0.08 g, 0.54 mmol), in THF (2 mL), was added dropwise until the suspension was transformed into a solution. The solvent was reduced *in vacuo* to dryness to afford the product as a pale yellow solid (0.26 g, 0.45 mmol, 83 %). ^{1}H NMR (400.20 MHz, d_8-THF, 298 K) 8.00 (s, 2H, ***HC=N***) 6.74 (dd, 2H, ^3J = 7.61 Hz, ^4J = 1.55 Hz, Ph**H**) 6.66 (dd, 2H, ^3J = 8.00 Hz, ^4J = 1.48 Hz, Ph**H**) 6.28 (t, 2H, ^3J = 7.80 Hz, Ph**H**) 3.81 (s, 6H, -OC**H**$_3$) 0.94 (s, 6H, -C(C**H**$_3$)$_2$). Methylene protons not observed. ^{13}C{^{1}H} NMR (125.81 MHz, $CDCl_3$, 298 K) 169.2 (H**C**=N) 162.3 (*ipso*-**Ph**) 152.1 (*o*-**Ph**-OCH$_3$) 127.5 (*m*-**Ph**-CH=N) 118.8 (*o*-**Ph**-CH=N) 112.2 (p-**Ph**) 111.2 (*m*-**Ph**) 75.1 (N-**C**H$_2$-C(CH$_3$)$_2$) 55.4 (-O**C**H$_3$) 35.3 (-**C**(CH$_3$)$_2$), Methyl signal not observed. Elemental Analysis for $C_{21}H_{24}IN_2NaO_4Zn$ (583.46 $gmol^{-1}$): Calculated; C, 43.2; H, 4.4; N, 4.8 %. Found; C, 43.1; H, 4.5; N, 4.8 %

Complex 5: $ZnEt_2$ (0.17 g, 1.35 mmol) was added dropwise to a solution of H_2L (0.50 g, 1.35 mmol), in THF (5 mL), and allowed to stir at 25 °C for 16 h. CaI_2 (0.40 g, 1.35 mmol), in THF (12 mL), was added dropwise and the pale yellow precipitate changed to a bright yellow suspension. The mixture was filtered and the solvent evacuated *in vacuo* to dryness to afford the product as a yellow powder (0.73 g, 1.01 mmol, 75 %). ^{1}H NMR (400.20 MHz, d_8-THF,

298 K) 8.16 (s, 2H, ***HC=N***) 7.07 (dd, 2H, ^3J = 7.89 Hz, ^4J = 1.55 Hz, Ph**H**) 6.86 (dd, 2H, ^3J = 7.61 Hz, ^4J = 1.48 Hz, Ph**H**) 6.57 (t, 2H, ^3J = 7.89 Hz, Ph**H**) 4.44 (br. 2H, N-C$\mathbf{H}_2$) 4.36 (s, 6H, -OC$\mathbf{H}_3$) 3.14 (br., 2H, N-C$\mathbf{H}_2$) 1.06 (s, 3H, -C(C$\mathbf{H}_3$)$_2$) 0.86 (br., 3H, -C(C$\mathbf{H}_3$)$_2$). ^{13}C{^{1}H} NMR (125.81 MHz, $CDCl_3$, 298 K) 170.2 (H**C**=N) 158.2 (*ipso*-**Ph**) 151.5 (*o*-**Ph**-OCH$_3$) 128.5 (*m*-**Ph**-CH=N) 119.0 (*o*-**Ph**-CH=N) 114.7 (p-**Ph**) 114.5 (*m*-**Ph**) 74.8 (N-**C**H$_2$-C(CH$_3$)$_2$) 60.3 (-O**C**H$_3$) 35.1 (-**C**(CH$_3$)$_2$), Methyl signal not observed. Elemental Analysis for $C_{21}H_{24}CaI_2N_2O_4Zn$ (725.87 gmol^{-1}): Calculated; C, 34.7; H, 3.3; N, 3.9 %. Found; C, 34.2; H, 3.1; N, 4.1 %.

Complex 6: $ZnEt_2$ (0.10 g, 0.81 mmol) was added dropwise to a solution of H_2L (0.30 g, 0.81 mmol), in THF (5 mL), and stirred at 25 °C for 4 h. CdI_2 (0.30 g, 0.81 mmol) was added and the suspension dissolved temporarily but upon further stirring (~10 mins) a precipitate formed. The mixture was filtered and the solid washed with pentane (2 x 5 mL). The combined filtrate was dried *in vacuo* to afford the product as a pale yellow solid (0.54 g, 0.68 mmol, 84 %). ^{1}H NMR (400.20 MHz, $CDCl_3$, 298 K) 8.05 (br. s, 2H, **H**C=N) 6.82 (d, 2H, ^3J = 7.54 Hz, Ph**H**) 6.71 (d, 2H, ^3J = 7.54 Hz, Ph**H**) 6.61 (t, 2H, ^3J = 7.54 Hz, Ph**H**) 3.84 (s, 6H, -OC$\mathbf{H}_3$) 3.66 (Br. s, 4H, N-C$\mathbf{H}_2$) 1.04 (s, 6H, -C(C$\mathbf{H}_3$)$_2$). ^{13}C{^{1}H} NMR (125.81 MHz, $CDCl_3$, 298 K): 171.6 (H**C**=N) 157.1 (*ipso*-**Ph**) 148.9 (*o*-**Ph**-OCH$_3$) 126.6 (m-**Ph**-CH=N) 117.2 (*o*-**Ph**-CH=N) 115.7 (*p*-**Ph**) 114.2 (*m*-**Ph**) 74.9 (N-**C**H$_2$-C(CH$_3$)$_2$) 54.3 (-O**C**H$_3$) 35.0 (-**C**(CH$_3$)$_2$) 24.6 (-C(**C**H$_3$)$_2$). Elemental analysis for $C_{21}H_{24}CdI_2N_2O_4Zn$ (800.03 gmol^{-1}): Calculated; C, 31.5; H, 3.0; N, 3.5 % Found; C,31.2; H, 3.3; N, 3.2 %.

Complex 7: Mg(N{Si(CH$_3$)$_3$}$_2$)$_2$ (0.19 g, 0.54 mmol) was added to a solution of H_2L (0.30 g, 0.54 mmol), in THF (5 mL), and stirred for 2 h. $MgBr_2$ (0.10 g, 54 mmol) was added and the solution was stirred for a further 16 h. The solution was reduced in *vacuo* to dryness and the crude product was washed with pentane (3 x 5 mL) to afford the product as a white solid (0.70 g, 1.22 mmol, 90 %). ^{1}H NMR (d_8-THF, 400.20 MHz, 298 K) 8.22 (s, 2H, **H**C=N) 6.98 (d, 2H, ^3J = 7.41 Hz, ortho-Ph**H**) 6.87 (d, 2H, ^3J = 7.41 Hz, meta-Ph**H**) 6.62 (t, 2H, ^3J = 7.66 Hz, para-Ph**H**) 4.07 (s, 6H, -OC$\mathbf{H}_3$) 3.79 (br. s, 4H, -C$\mathbf{H}_2$) 0.98 (s, 6H, -C$\mathbf{H}_3$). ^{13}C{^{1}H} NMR (d_8-THF, 125.81 MHz, 298 K) 170.4 (H**C**=N) 154.9 (*ipso*-**Ph**) 150.8 (*o*-**Ph**-OCH$_3$) 127.2 (*m*-**Ph**-CH=N) 120.2 (*o*-**Ph**-CH=N) 115.8 (*p*-**Ph**) 113.8 (*m*-**Ph**-OCH$_3$) 74.5 (N-**C**H$_2$-C(CH$_3$)$_2$) 56.2 (-O**C**H$_3$) 35.8 (-**C**(CH$_3$)$_2$) 26.2 (-C(**C**H$_3$)$_2$). Elemental Analysis for $C_{21}H_{24}Br_2Mg_2N_2O_4$ (573.98 gmol^{-1}): Calculated; C, 43.7; H, 4.2; N, 4.9 %. Found: C, 43.8; H, 4.3; N, 4.7 %.

Complex 9: Mg(N{Si(CH$_3$)$_3$}$_2$)$_2$ (0.19 g, 0.54 mmol) was added to a solution of H_2L (0.30 g, 0.54 mmol), in THF (5 mL), and stirred for 2 h. NaI (0.08 g, 54 mmol) was added and the solution was stirred for a further 16 h. The solution was reduced in *vacuo* to dryness and the crude product was washed with pentane (3 x 5 mL) to afford the product as a white solid (0.26 g, 0.45 mmol, 83 %) ^{1}H NMR (400.20 MHz, d_8-THF, 298 K) 8.18 (s, 2H, ***HC=N***) 6.78 (dd, 2H, ^3J = 7.61 Hz, ^4J = 1.55 Hz, Ph**H**) 6.72 (dd, 2H, ^3J = 8.00 Hz, ^4J = 1.48 Hz, Ph**H**) 6.35 (t, 2H, ^3J = 7.80 Hz, Ph**H**) 3.97 (s, 6H, -OC$\mathbf{H}_3$) 1.03 (s, 6H, -C(C$\mathbf{H}_3$)$_2$). Methylene protons not observed. ^{13}C{^{1}H} NMR (125.81 MHz, d_8-THF, 298 K) 169.2 (H**C**=N) 162.3 (*ipso*-**Ph**) 152.1 (*ortho*-**Ph**) 127.5 (*ortho*-**Ph**) 118.8 (*meta*-**Ph**) 112.2 (*meta*-**Ph**) 111.2 (*para*-**Ph**) 75.1 (N**C**H$_2$C(CH$_3$)$_2$) 55.4 (-O**C**H$_3$) 35.3 (NCH$_2$**C**(CH$_3$)$_2$). Methyl signal not observed. Elemental Analysis for $C_{21}H_{24}IN_2NaO_4Zn$ (583.46 gmol^{-1}): Calculated; C, 46.5; H, 4.5; N, 5.2 % Found; C, 46.2; H, 4.6; N, 5.1 %.

Complex 10: Mg(N{Si(CH$_3$)$_3$}$_2$)$_2$ (0.19 g, 0.54 mmol) was added to a solution of H_2L (0.30 g, 0.54 mmol), in THF (5 mL), and stirred for 2 h. CaI_2 (0.16 g, 54 mmol) was added and the solution was stirred for a further 16 h. The solution was reduced in *vacuo* to dryness and the crude product was washed with pentane (3 x 5 mL) to afford the product as a white solid (0.22 g, 0.39 mmol, 72 %) ^{1}H NMR (400.20 MHz, d_8-THF, 298 K) 8.24 (s, 2H, ***HC=N***) 7.11 (d, 2H, ^3J = 8.40 Hz, Ph**H**) 6.94 (d, 2H, ^3J = 8.00 Hz, Ph**H**) 6.62 (t, 2H, ^3J = 8.40 Hz, Ph**H**) 4.35 (s, 6H, -OC$\mathbf{H}_3$) 3.83 (br. 4H, -C$\mathbf{H}_2$C(CH$_3$)$_2$) 0.95 (s, 6H, -C(C$\mathbf{H}_3$)$_2$). ^{13}C{^{1}H} NMR (125.81 MHz, d_8-THF, 298 K) 169.8 (H**C**=N) 155.6 (*ipso*-**Ph**) 150.6 (*ortho*-**Ph**) 127.7 (*ortho*-**Ph**) 119.8 (*meta*-**Ph**) 114.4 (*meta*-**Ph**) 114.0 (*para*-**Ph**) 74.1 (N**C**H$_2$C(CH$_3$)$_2$) 59.0 (-O**C**H$_3$) 34.8 (NCH$_2$**C**(CH$_3$)$_2$). Elemental Analysis for $C_{21}H_{24}CaI_2MgN_2O_4$ (685.93 gmol^{-1}): Calculated; C, 36.7; H, 3.5; N, 4.1 % Found; C, 37.3; H, 3.3; N, 4.3 %.

Complex 11: Mg(N{Si(CH$_3$)$_3$}$_2$)$_2$ (0.19 g, 0.54 mmol) was added to a solution of H_2L (0.30 g, 0.54 mmol), in THF (5 mL), and stirred for 2 h. CdI_2 (0.20 g, 54 mmol) was added and the solution was stirred for a further 16 h. The solution was reduced in *vacuo* to dryness and the crude product was washed with pentane (3 x 5 mL) to afford the product as a white solid (0.27 g, 0.35 mmol, 65 %) ^{1}H NMR (400.20 MHz, $CDCl_3$, 298 K) 7.99 (br., 2H, ***HC=N***) 6.76 (d, 2H, ^3J = 7.41 Hz, Ph**H**) 6.65 (d, 2H, ^3J = 7.81 Hz, Ph**H**) 6.54 (t, 2H, ^3J = 7.81 Hz, Ph**H**) 3.78 (s, 6H, -OC$\mathbf{H}_3$) 3.60 (br. 4H, -C$\mathbf{H}_2$C(CH$_3$)$_2$) 0.97 (s, 6H, -C(C$\mathbf{H}_3$)$_2$). ^{13}C{^{1}H} NMR (125.81 MHz, $CDCl_3$, 298 K) 172.3 (H**C**=N) 155.6 (*ipso*-**Ph**) 149.4 (*o*-**Ph**) 126.6 (*o*-**Ph**) 119.0 (*m*-**Ph**) 115.8 (*m*-**Ph**) 114.6 (*p*-**Ph**) 75.4 (N**C**H$_2$C(CH$_3$)$_2$) 54.5 (-O**C**H$_3$) 35.7 (NCH$_2$**C**(CH$_3$)$_2$) 24.9 (NCH$_2$C(**C**H$_3$)$_2$). Elemental Analysis for $C_{21}H_{24}CdI_2MgN_2O_4$ (759.87 gmol^{-1}): Calculated; C, 33.2; H, 3.2; N, 3.7 %. Found; C, 32.8; H, 3.4; N, 4.1 %.

General procedure for PA/CHO ROCOP Catalysis

The catalyst (15 µmol, typical weight 10-15 mg) and phthalic anhydride (220 mg, 1.5 mmol) was dissolved in CHO (1.5 mL, 15 mmol) under N_2 and heated to 100 ˚C. Aliquots were taken and quenched with wet chloroform and exposed to air. Reaction conversion was determined by ^{1}H NMR spectroscopy and the polymer molecular mass was measured via GPC analysis.

Crystallographic details

The molecular structures of **1**-**8**, **10**, **11**, **A** and **B** were solved using SHELXT[1] and least-square refined using SHELXL[2] in Olex2[3] or WinGX.[4] Hydrogen atoms were treated by constrained refinement. **2** – was refined as 2 component inversion twin with a ratio of 0.58:0.42. C(22)/C(23)/C(24)/C(25) were positionally disordered over two positions and were split into two parts and refined with an occupancy ratio of 0.68:0.32. C(2A)/C(3A)/C(4A) were positionally disordered over two positions and were split into two parts and refined with an occupancy ratio of 0.64:0.36. O(1C)/C(2C)/C(3C)/C(4C)/C(5C) were positionally disordered over two positions and were split into two parts and refined with an occupancy ratio of 0.62:0.38. In addition, the thermal parameters were restrained using the RIGU command and the bond angles were restrained through the use of the SADI command for coordinated and solvent THF molecules. In addition, the thermal parameters were constrained to be equal for the coordinated and solvent THF by use of the EADP and EXYZ command. **4**· – C(22)/C(23)/C(24) were positionally disordered over two positions and were split into two parts and refined with an occupancy ratio of 0.68:0.32. C(30)/C(31)/C(32) were positionally disordered over two positions and were split into two parts and refined with an occupancy ratio of 0.53:0.47. In addition, the thermal parameters were set to be similar by use of the SIMU command and restrained using the RIGU command. In addition, the thermal parameters were constrained to be equal for the split C(22), C(23), C(24), C(30), C(31) and C(32) by use of the EADP and EXYZ command. **5**· – C(22)/C(23)/C(24)/C(25) were positionally disordered over two positions and were split into two parts and refined with an occupancy ratio of 0.56:0.44. C(27)/C(28)/C(29) were positionally disordered over two positions and were split into two parts and refined with an occupancy ratio of 0.53:0.47. O(7)/C(90)/C(91)/C(92)/C(93) were positionally disordered over two positions and were split into two parts and refined with an occupancy ratio of 0.35:0.65. In addition, the thermal parameters were set to be similar by use of the SIMU command, restrained using the RIGU command and the bond angles were restrained through the use of the SADI command for coordinated and solvent THF molecules. In addition, the thermal parameters were constrained to be equal for the split C(27) and C(29) by use of the EADP and EXYZ command. **11** – The Olex solvent mask feature[1] was used to remove 188 electrons from solvent accessible voids, which equates to approximately 2 hexane and 2 acetonitrile molecules.

CCDC numbers: 2057256 - 2057267

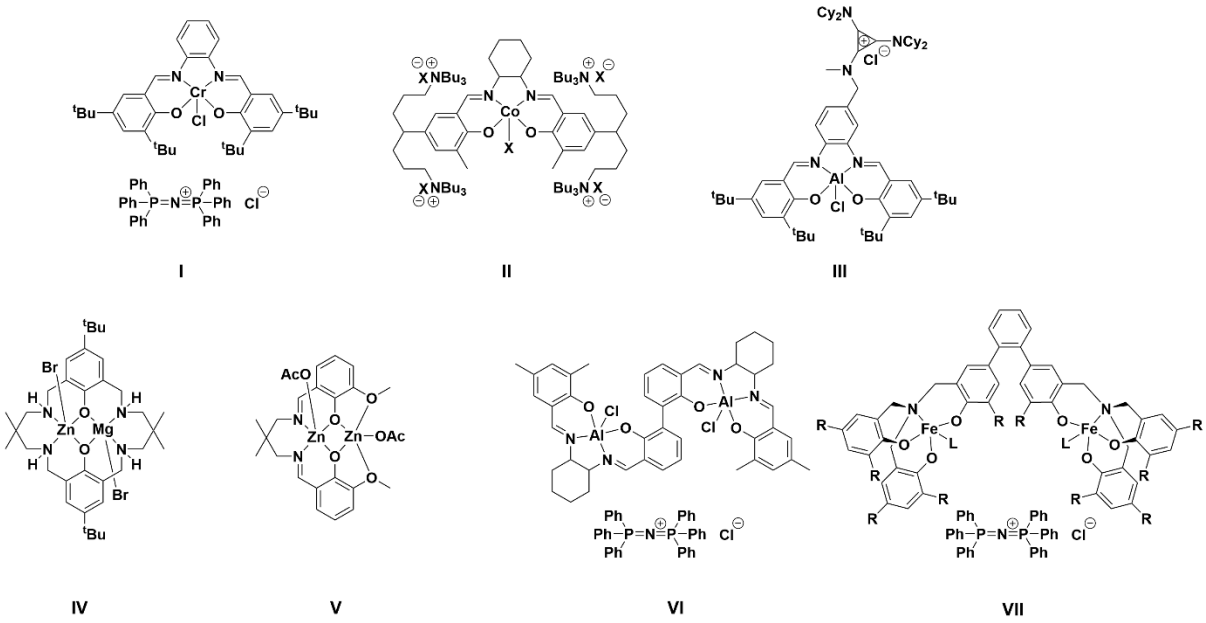

Figure S1: A selection of reported catalysts for anhydride/epoxide ROCOP.[5-10]

2

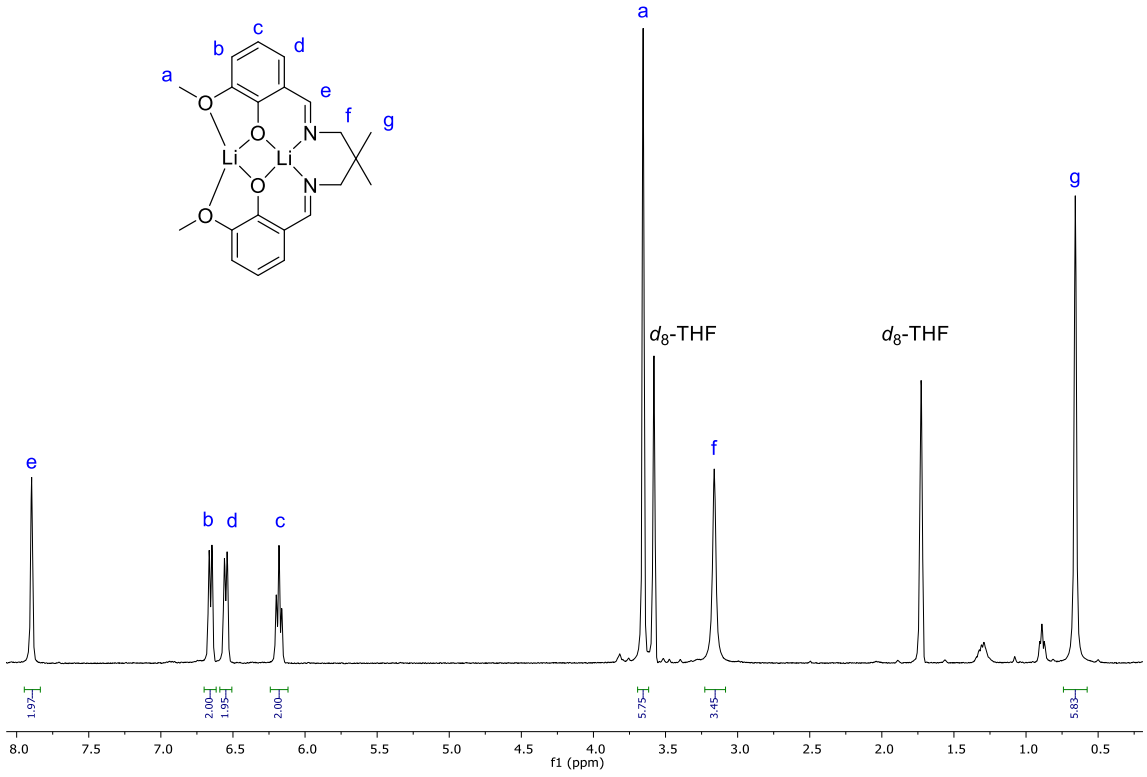

Figure S2: ^{1}H NMR spectrum of (**1**) (d_8-THF, 298 K).

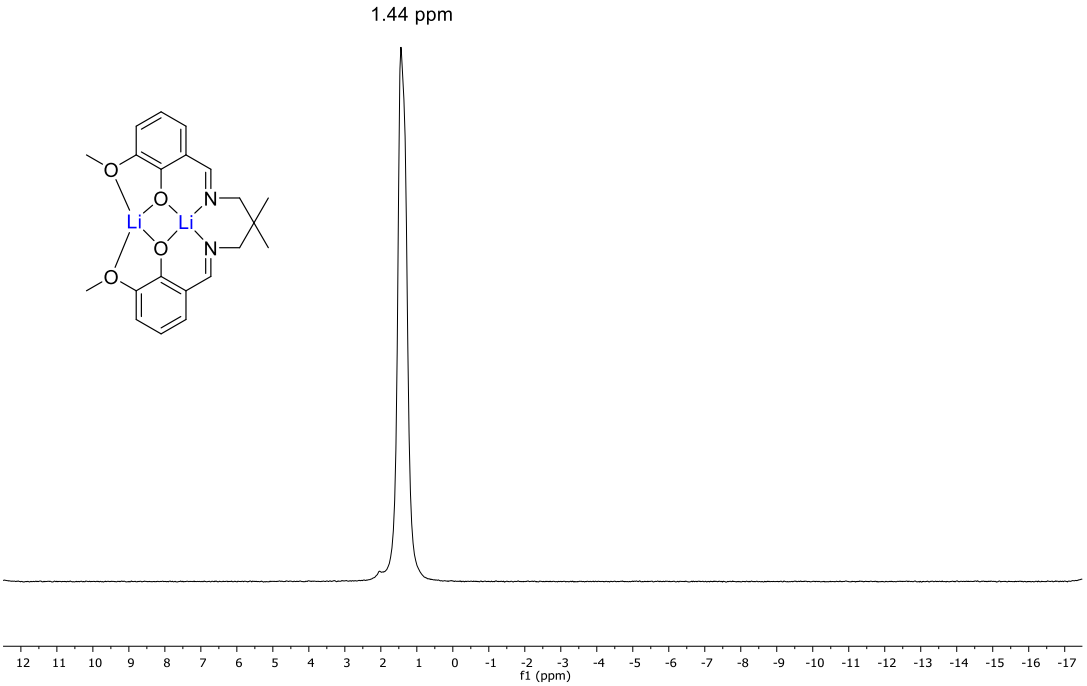

Figure S3: ^{7}Li NMR spectrum of (**1**) (d_8-THF, 298 K).

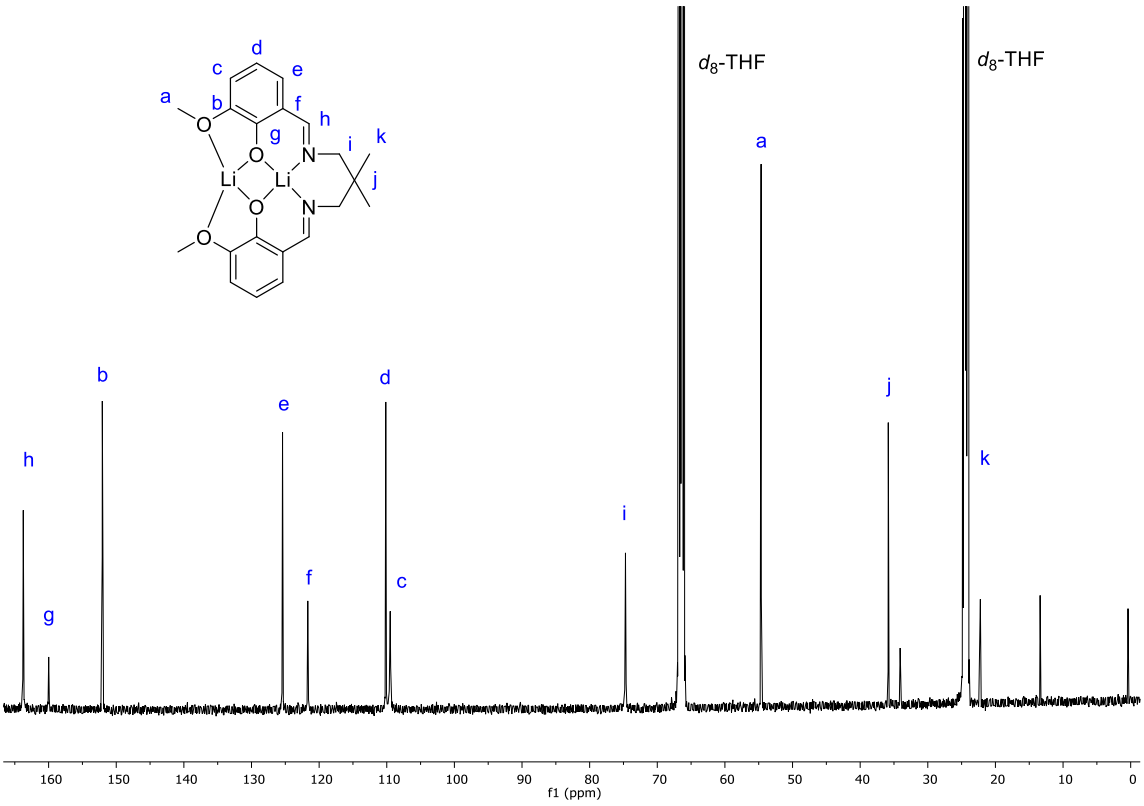

Figure S4: ^{13}C{^{1}H} NMR spectrum of (**1**) (d_8-THF, 298 K).

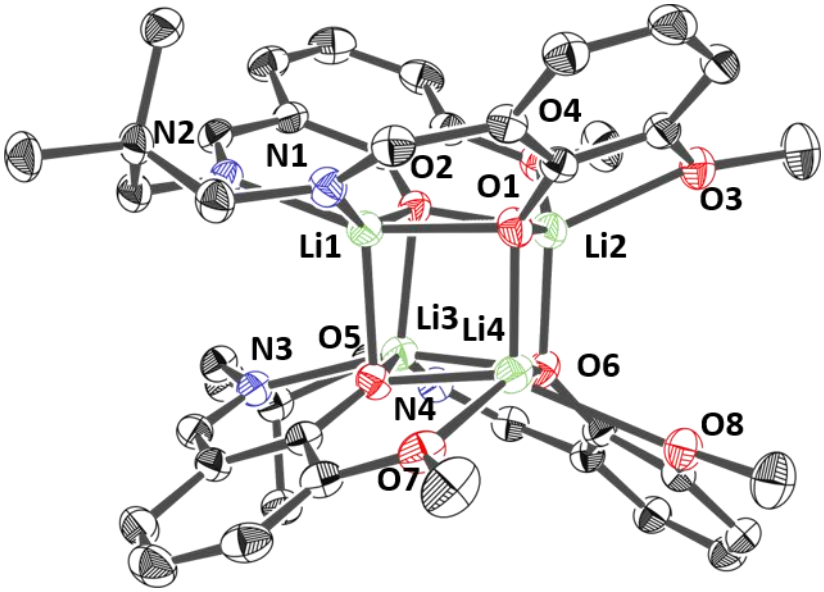

Figure S5: ORTEP representation of the molecular structure of (**1**), with disorder and hydrogen atoms omitted for clarity and thermal ellipsoids represented at 40 % probability.

Table S1: Selected bond lengths (Å) and angles (°) for complex (**1**).

Bond	Bond Length (Å)	Bond	Bond Angle (°)
N (1) – Li (1)	2.068(7)	N (1) – Li (1) – O (2)	155.6(3)
N (2) – Li (1)	2.109(7)	N (2) – Li (1) – O (1)	159.5(3)
O (1) – Li (1)	2.028(7)	N (1) – Li (1) – O (5)	109.9(3)
O (2) – Li (1)	1.937(7)	O (3) – Li (2) – O (2)	143.5(3)
O (5) – Li (1)	2.030(6)	O (4) – Li (2) – O (1)	150.2(4)
O (1) – Li (2)	1.962(7)	O (3) – Li (2) – O (6)	114.1(3)
O (2) – Li (2)	1.905(7)		
O (3) – Li (2)	2.491(7)	**Metal – Metal**	**Distance (Å)**
O (4) – Li (2)	2.386(8)		
O (6) – Li (2)	1.922(7)	Li (1) – Li (2)	2.840(9)

.

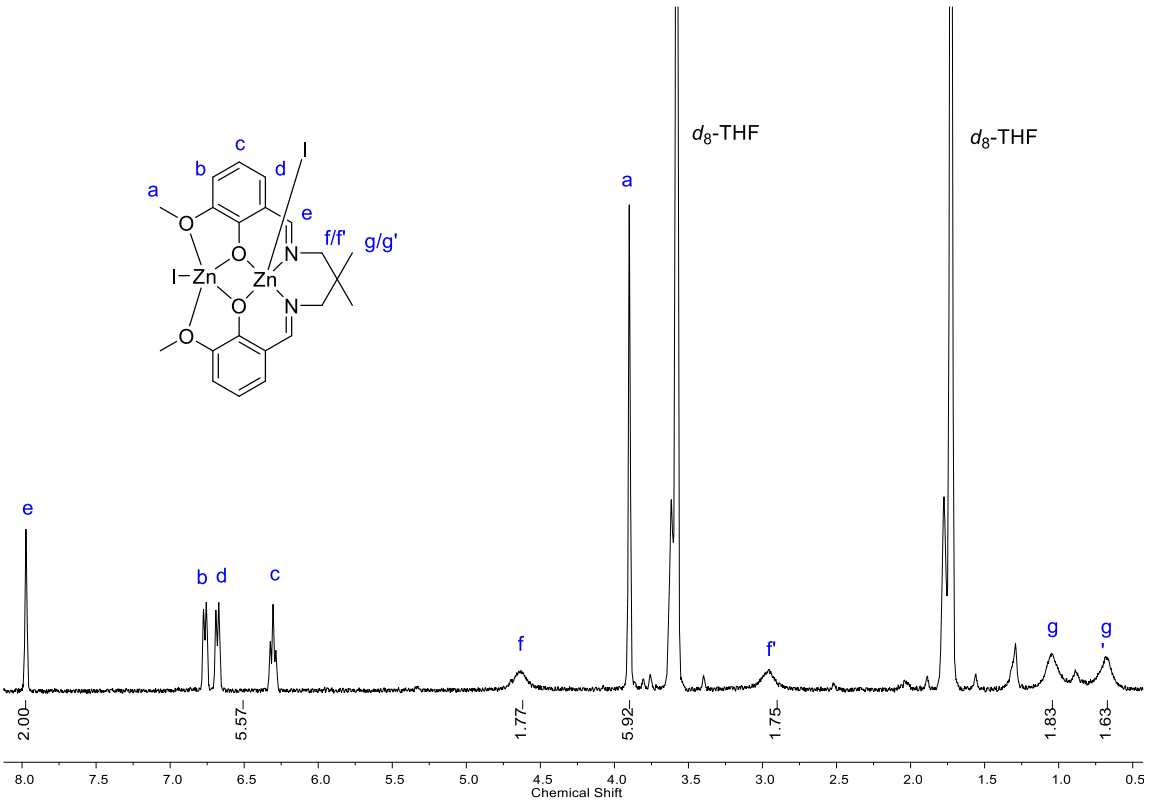

Figure S6: ^{1}H NMR spectrum of (**2**) (d_8-THF, 298 K).

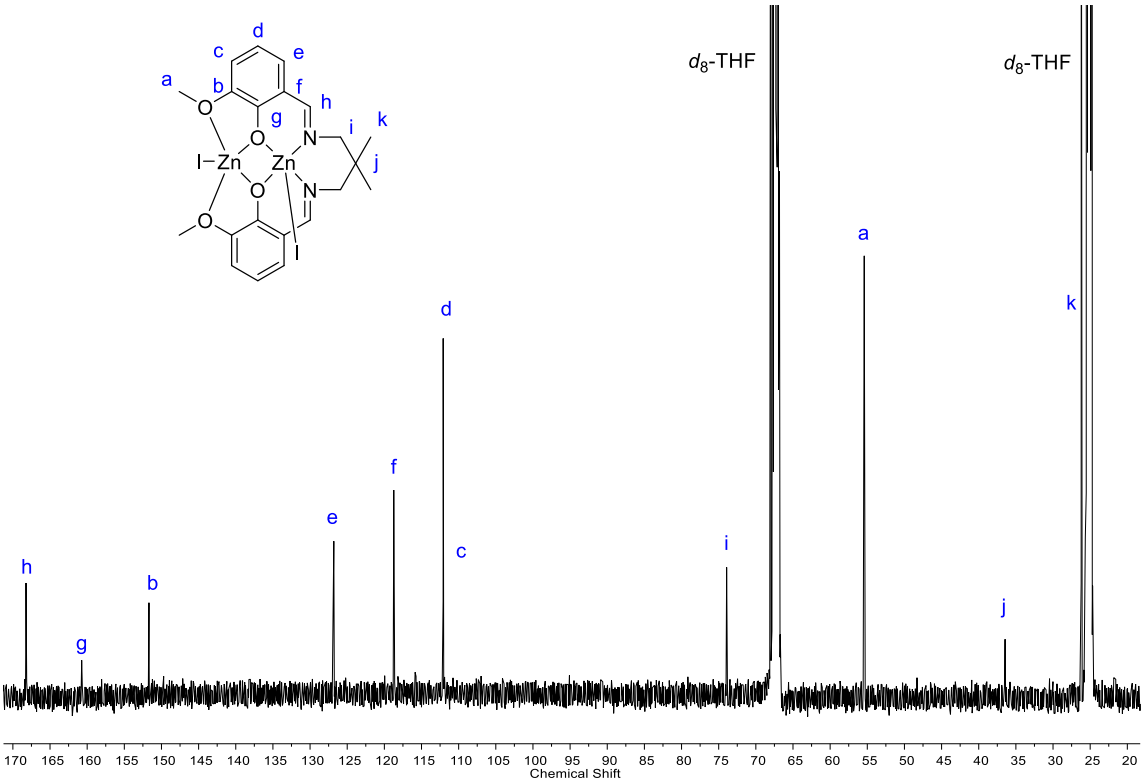

Figure S7: ^{13}C{^{1}H} NMR spectrum of (**2**) in (d_8-THF, 298 K).

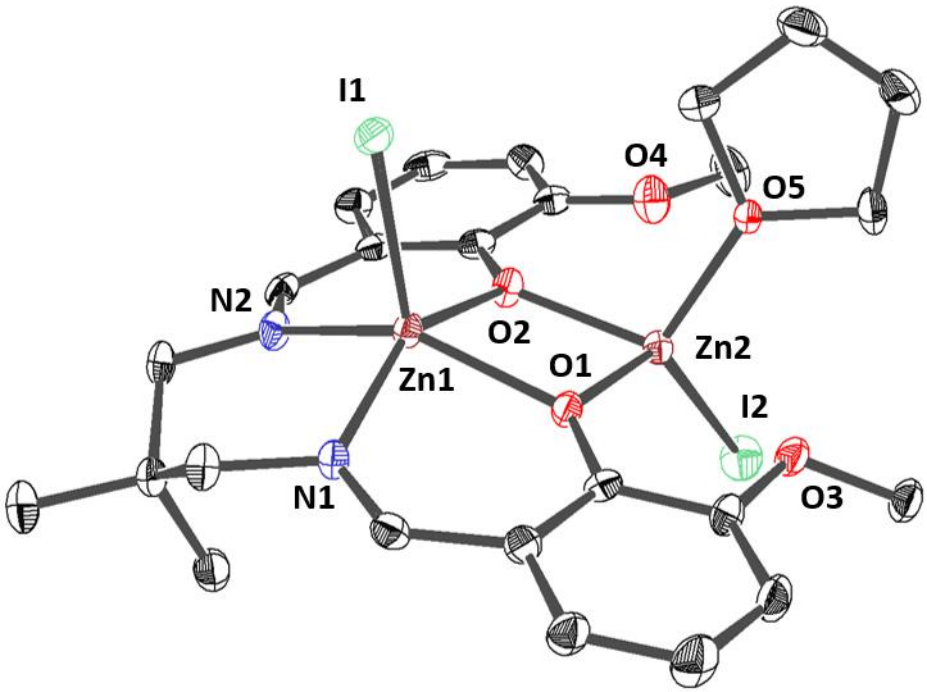

Figure S8: ORTEP representation of the molecular structure of (**2**), with disorder and hydrogen atoms omitted for clarity and thermal ellipsoids represented at 40 % probability.

Table S2: Selected bond lengths (Å) and angles (°) for complex (**2**).

Bond	**Bond Length (Å)**	**Bond**	**Bond Angel (°)**
N (1) – Zn (1)	2.076(5)	N (1) – Zn (1) – O (2)	150.0(3)
N (2) – Zn (1)	2.109(7)	N (2) – Zn (1) – O (1)	142.1(3)
O (1) – Zn (1)	2.082(6)	N (1) – Zn (1) – I (1)	101.0(2)
O (2) – Zn (1)	2.070(5)	O (1) – Zn (2) – O (5)	104.0(2)
I (1) – Zn (1)	2.63297(13)	O (2) – Zn (2) – I (2)	117.84(19)
O (1) – Zn (2)	1.995(6)	O (5) – Zn (2) – I (2)	118.96(18)
O (2) – Zn (2)	2.012(6)		
O (5) – Zn (2)	2.035(7)	**Metal – Metal**	**Distance (Å)**
I (2) – Zn (2)	2.5232(12)	Zn (1) – Zn (2)	3.21325(6)

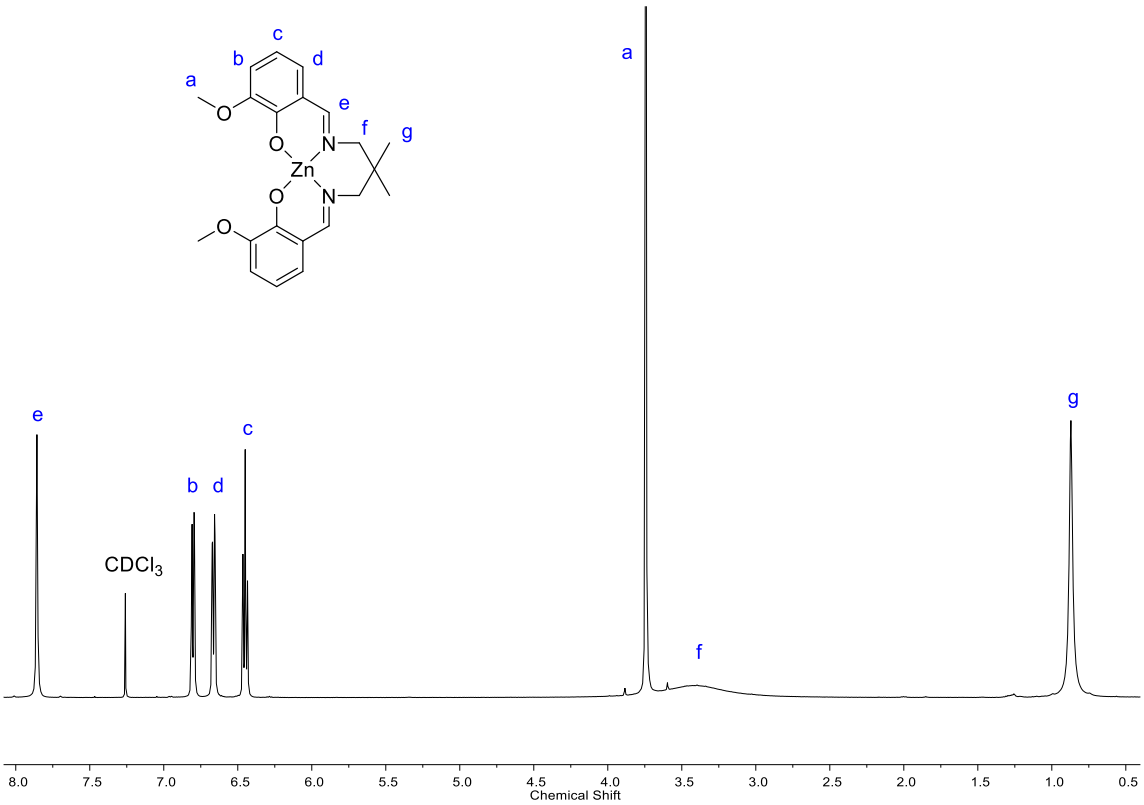

Figure S9: ^{1}H NMR spectrum of (**3**) ($CDCl_3$, 298 K).

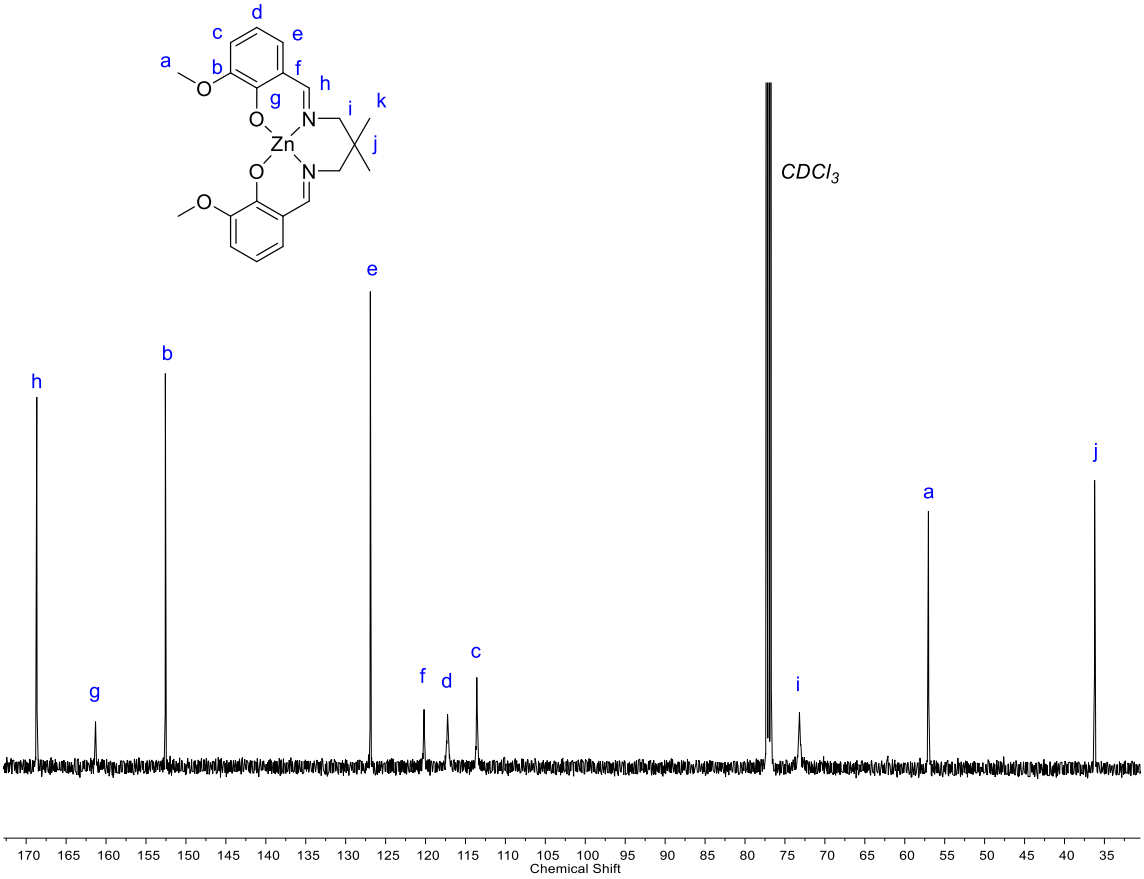

Figure S10: $^{13}C\{^{1}H\}$ NMR of (**3**) ($CDCl_3$, 298 K).

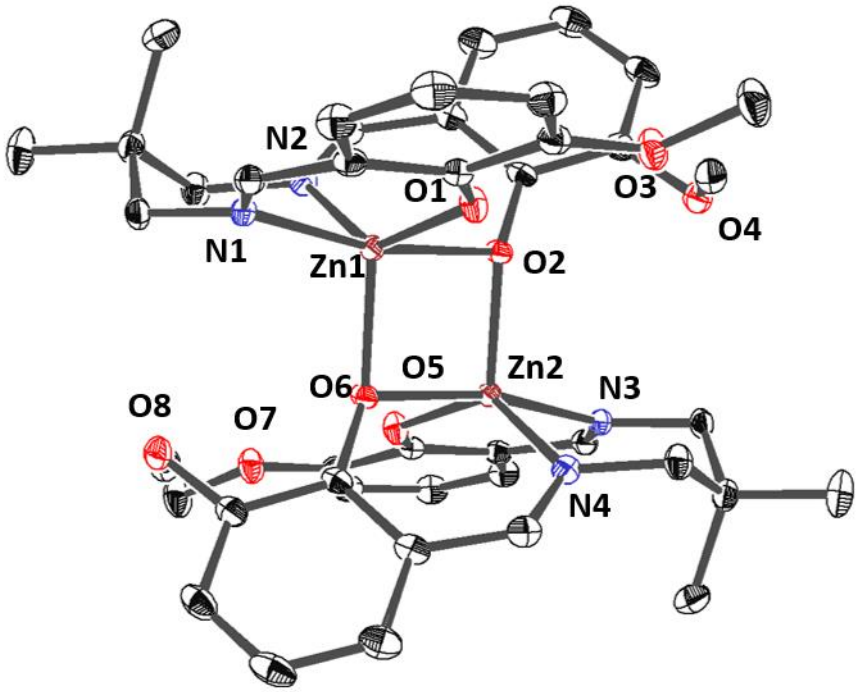

Figure S11: ORTEP representation of the molecular structure of (**3**), with disorder and hydrogen atoms omitted for clarity and thermal ellipsoids represented at 40 % probability.

Table S3: Selected bond lengths (Å) and angles (°) for complex (**3**).

Bond	**Bond Length (Å)**	**Bond**	**Bond Angel (°)**
N (1) – Zn (1)	2.0741(13)	N (1) – Zn (1) – O (2)	168.70(5)
N (2) – Zn (1)	2.0977(14)	N (2) – Zn (1) – O (1)	136.66(5)
O (1) – Zn (1)	1.9575(11)	N (1) – Zn (1) – O (6)	108.35(5)
O (2) – Zn (1)	2.1437(11)	N (3) – Zn (2) – O (6)	168.70(5)
O (6) – Zn (2)	2.0102(10)	N (4) – Zn (2) – O (5)	136.66(5)
N (2) – Zn (2)	2.0741(13)	N(3) – Zn (2) – O (2)	108.35(5)
N (3) – Zn (2)	2.0977(14)		
O (5) – Zn (2)	1.9575(11)	**Metal – Metal**	**Distance (Å)**
O (6) – Zn (2)	2.1437(11)		
O (2) – Zn (2)	2.0102(10)	Zn (1) – Zn (2)	3.1217(4)

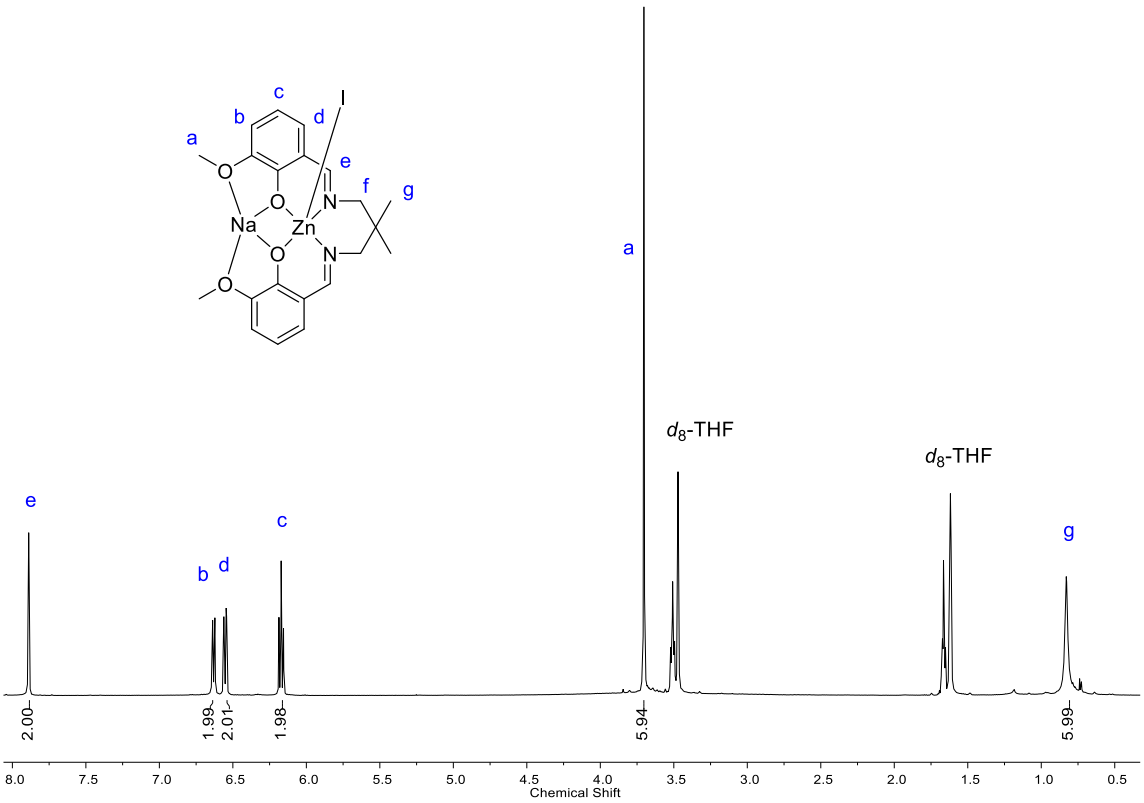

Figure S12: ^{1}H NMR spectrum of (**4**) (d_8-THF, 298 K).

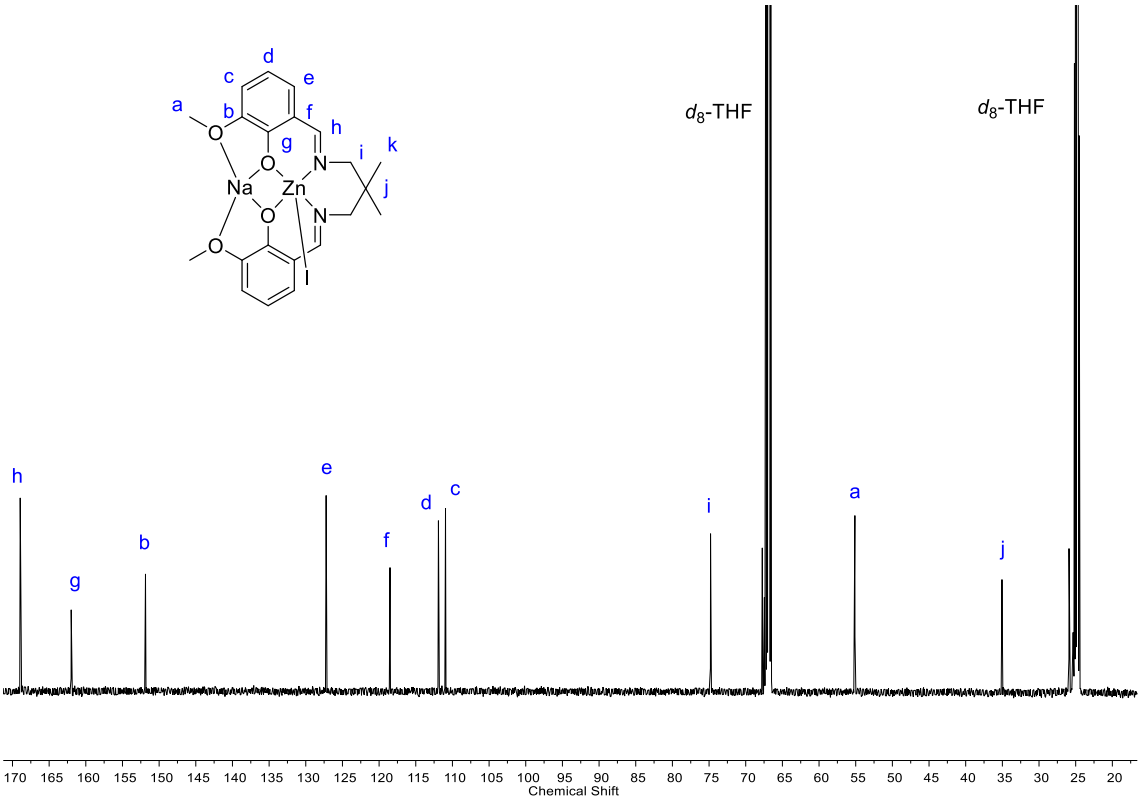

Figure S13: ^{13}C{^{1}H} NMR of (**4**) (d_8-THF, 298 K).

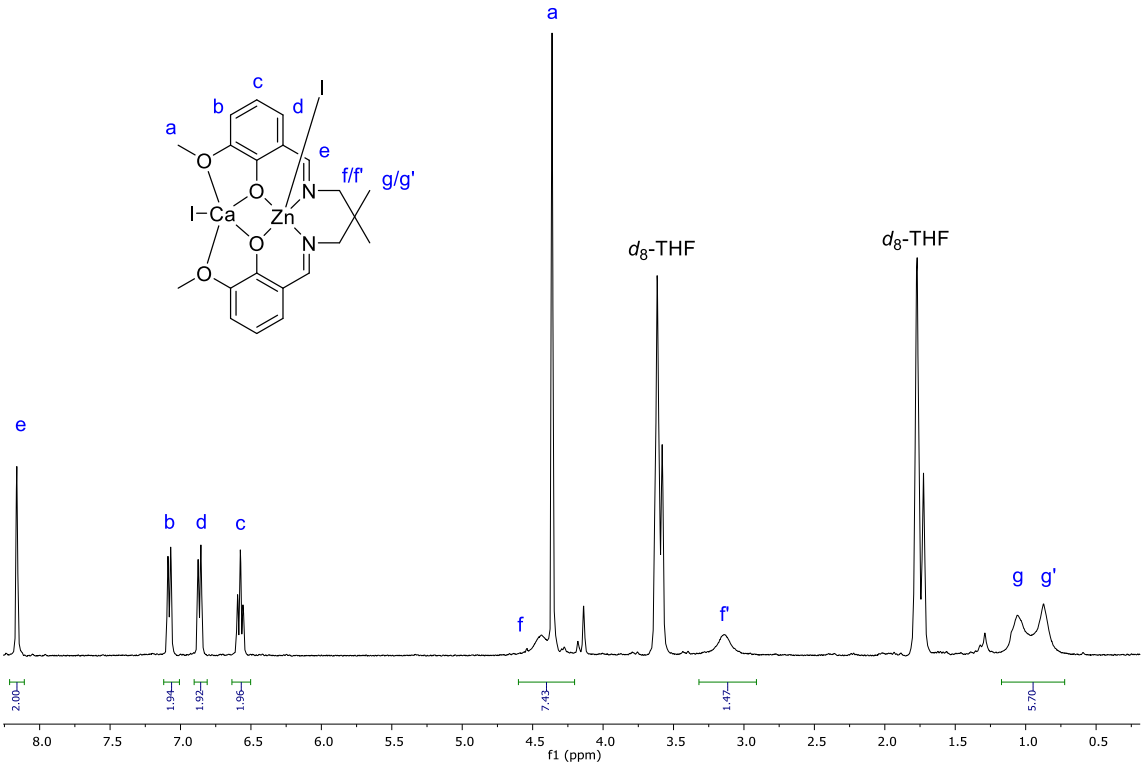

Figure S14: ^{1}H NMR spectrum of (**5**) (d_8-THF, 298 K).

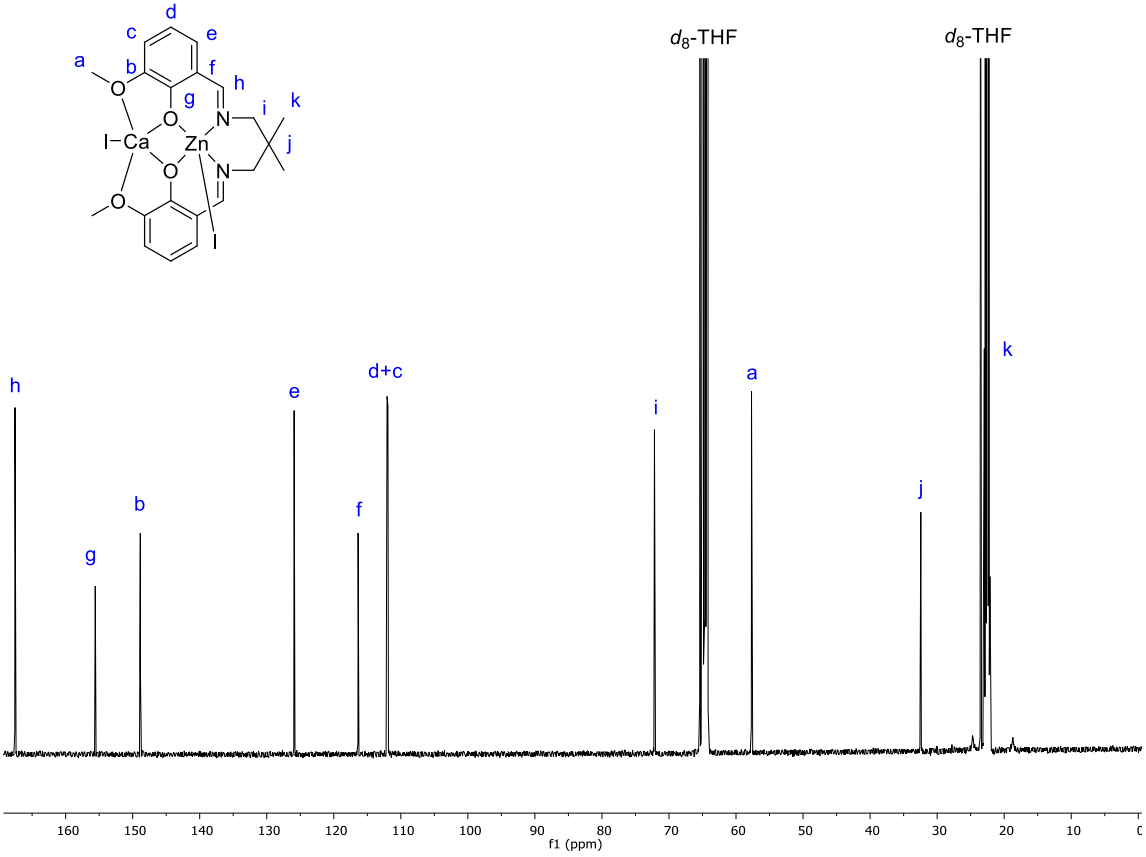

Figure S15: ^{13}C{^{1}H} NMR spectrum of (**5**) (d_8-THF, 298 K).

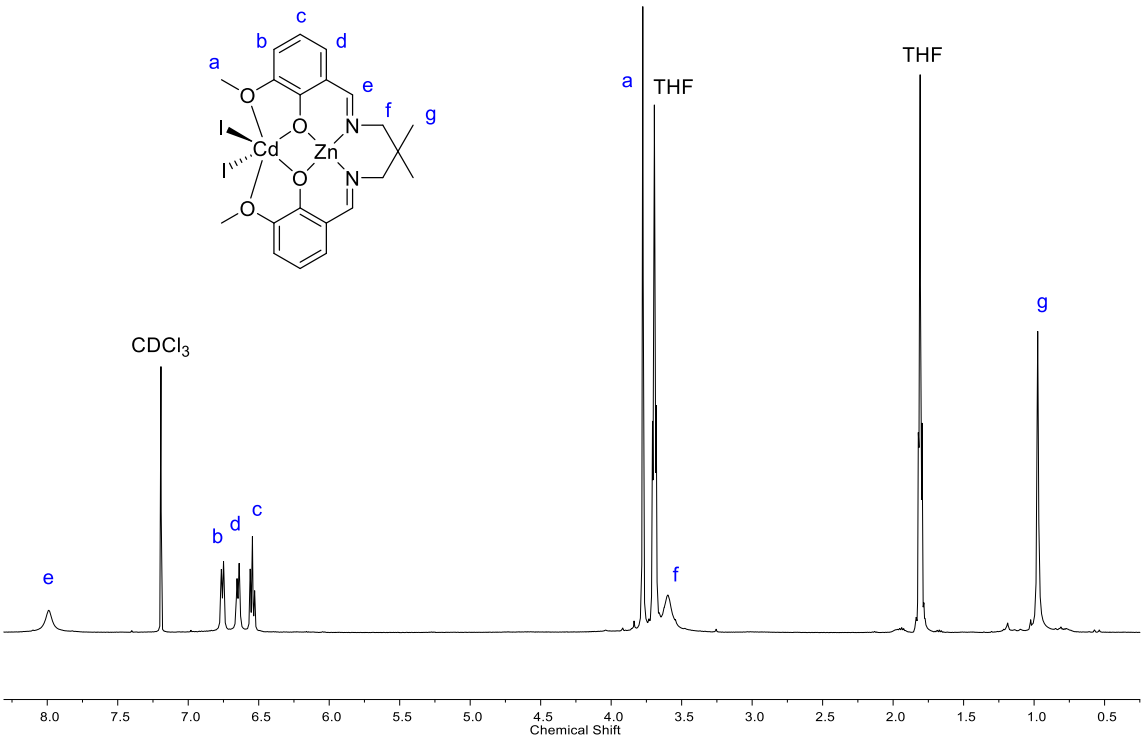

Figure S16: ^{1}H NMR spectrum of (**6**) ($CDCl_3$ 298 K).

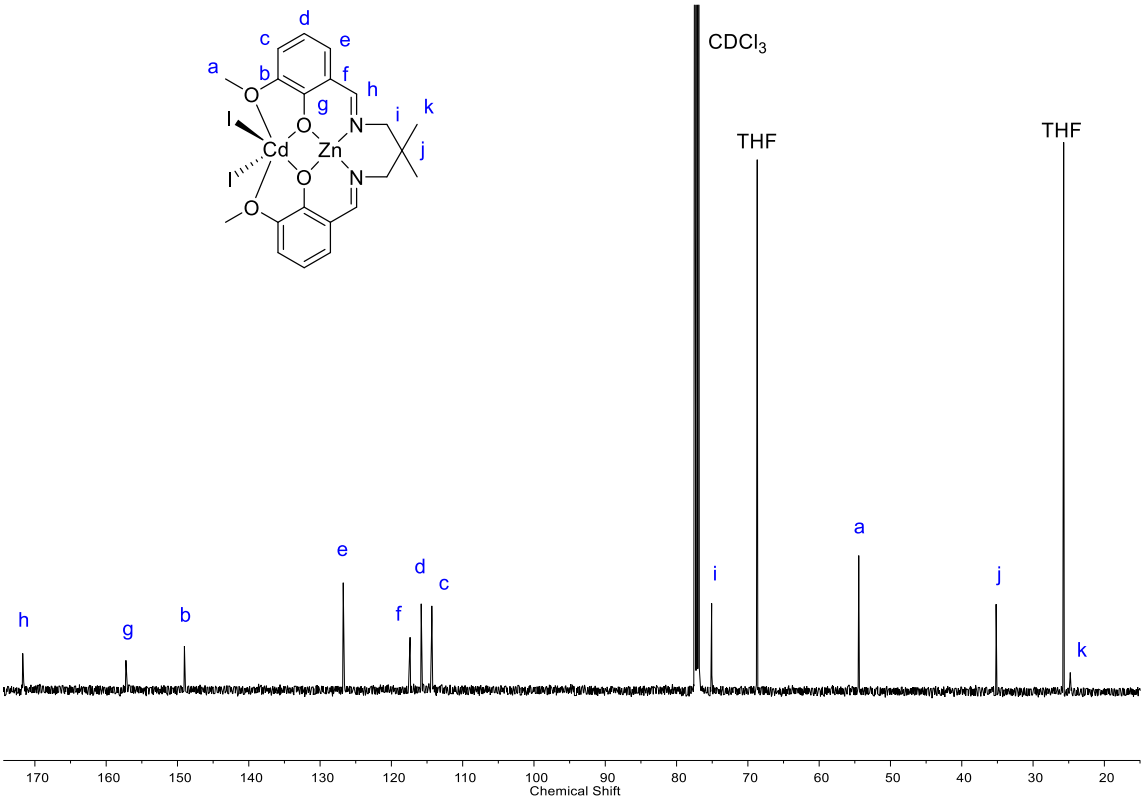

Figure S17: $^{13}C\{^{1}H\}$ NMR spectrum of (**6**) ($CDCl_3$. 298 K).

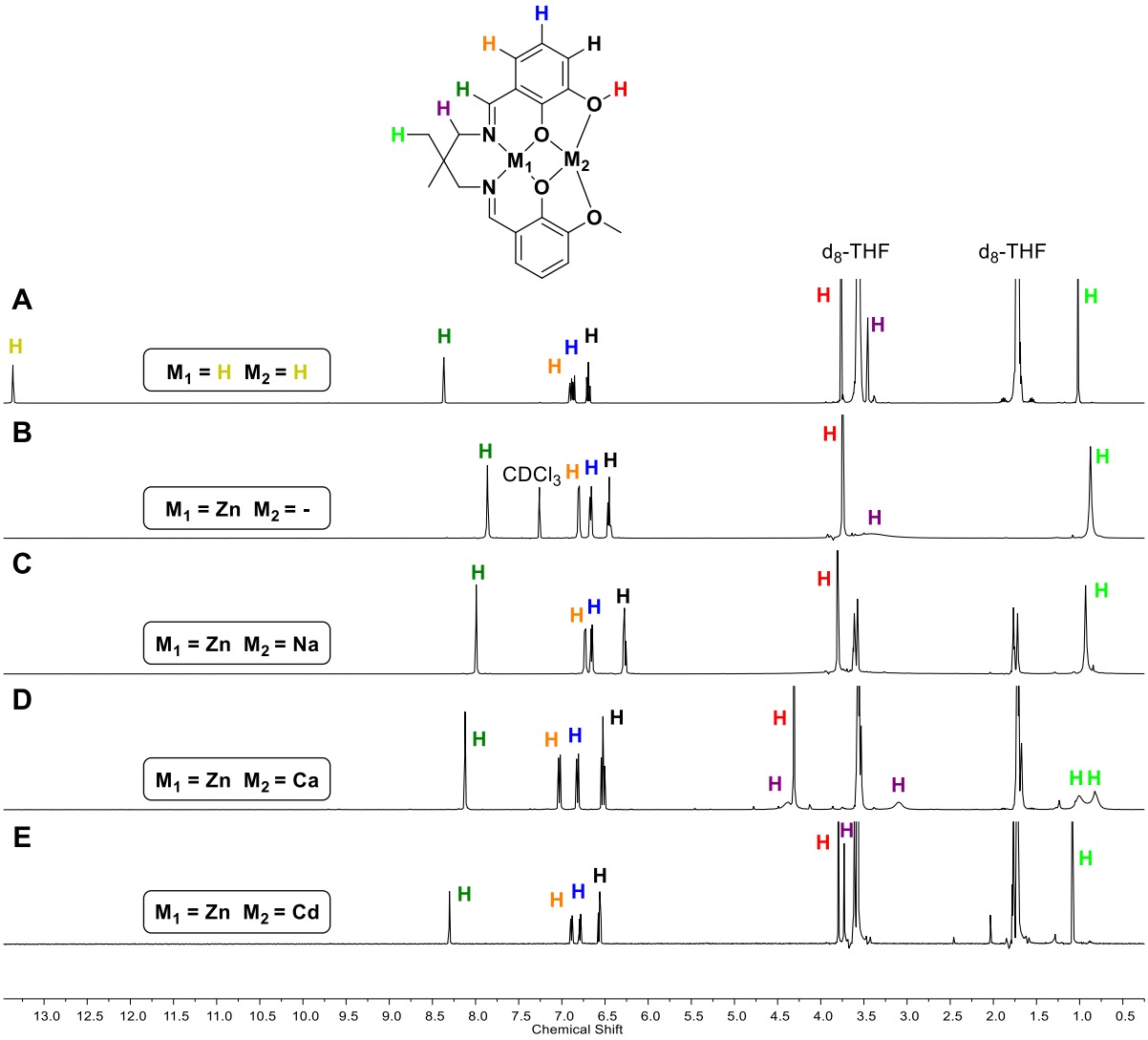

Figure S18: Stacked ^{1}H NMR spectrum plot of complexes (**3**-**6**) and pro-ligand **H_2L**.

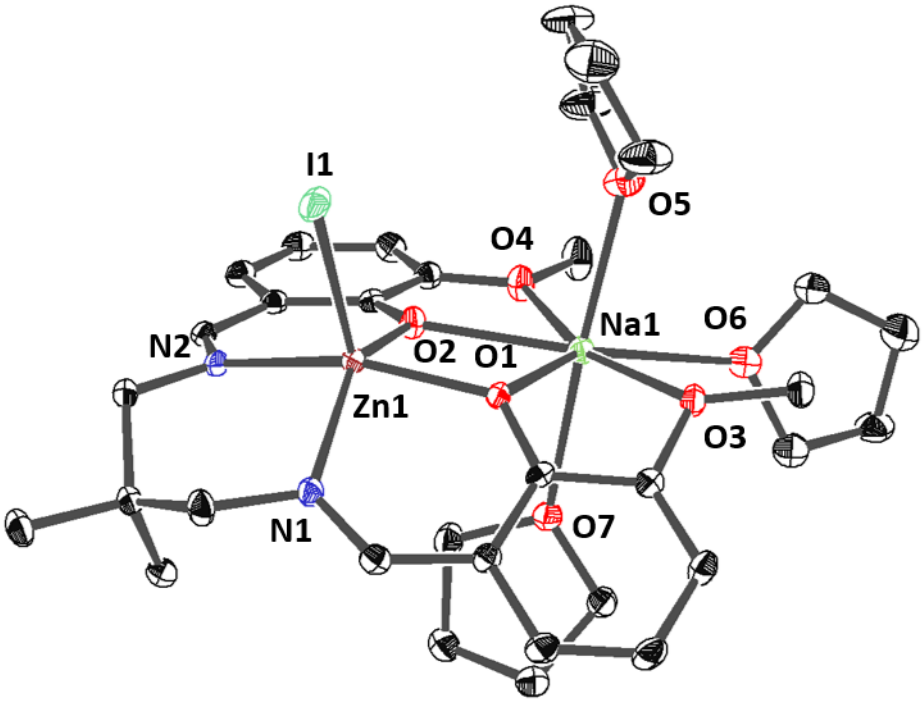

Figure S19: ORTEP representation of the molecular structure of (**4**), with disorder and hydrogen atoms omitted for clarity and thermal ellipsoids represented at 40 % probability.

Table S4: Selected bond lengths (Å) and angles (°) for complex (**4**).

Bond	**Bond Length (Å)**	**Bond**	**Bond Angel (°)**
N (1) – Zn (1)	2.115(2)	N (1) – Zn (1) – O (2)	141.55(10)
N (2) – Zn (1)	2.128(3)	N (2) – Zn (1) – O (1)	157.12(10)
O (1) – Zn (1)	2.009(2)	N (1) – Zn (1) – I (1)	102.59(7)
O (2) – Zn (1)	2.050(2)	O (1) – Na (1) – O (6)	141.66(10)
I (1) – Zn (1)	2.6560(5)	O (1) – Na (1) – O (5)	101.30(10)
O (1) – Na (1)	2.388(2)	O (5) – Na (1) – O (7)	173.91(11)
O (2) – Na (1)	2.376(3)		
O (3) – Na (1)	2.497(3)	**Metal – Metal**	**Distance (Å)**
O (4) – Na (1)	2.481(3)		
O (5) – Na (1)	2.450(3)	Zn (1) – Na (1)	3.5461(13)
O (6) – Na (1)	2.650(3)		
O (7) – Na (1)	2.481(3)		

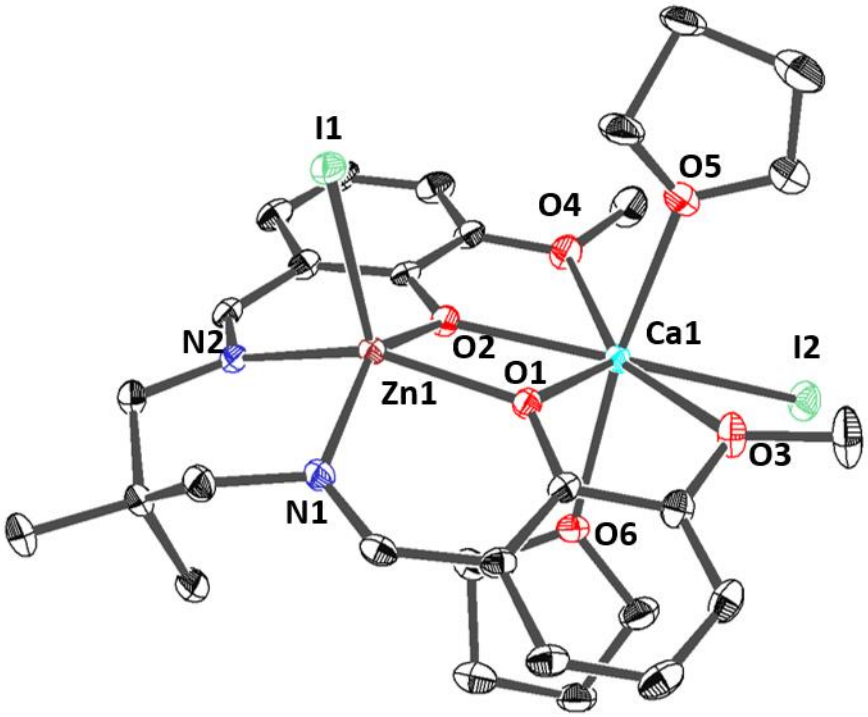

Figure S20: ORTEP representation of the molecular structure of (**5**), with disorder and hydrogen atoms omitted for clarity and thermal ellipsoids represented at 40 % probability.

Table S5: Selected bond lengths (Å) and angles (°) for complex (**5**).

Bond	**Bond Length (Å)**	**Bond**	**Bond Angel (°)**
N (1) – Zn (1)	2.086(3)	N (1) – Zn (1) – O (2)	144.18(11)
N (2) – Zn (1)	2.132(3)	N (2) – Zn (1) – O (1)	149.77(11)
O (1) – Zn (1)	2.083(2)	N (1) – Zn (1) – I (1)	104.20(9)
O (2) – Zn (1)	2.043(2)	O (1) – Ca (1) – I (2)	144.46(6)
I (1) – Zn (1)	2.6313(5)	O (1) – Ca (1) – O (5)	95.22(11)
O (1) – Ca (1)	2.357(2)	O (5) – Ca (1) – O (7)	170.314(12)
O (2) – Ca (1)	2.333(2)		
O (3) – Ca (1)	2.502(3)	**Metal – Metal**	**Distance (Å)**
O (4) – Ca (1)	2.482(3)		
O (5) – Ca (1)	2.365(3)	Zn (1) – Ca (1)	3.5785(8)
O (6) – Ca (1)	2.401(3)		
I (2) – Ca (1)	3.1686(7)		

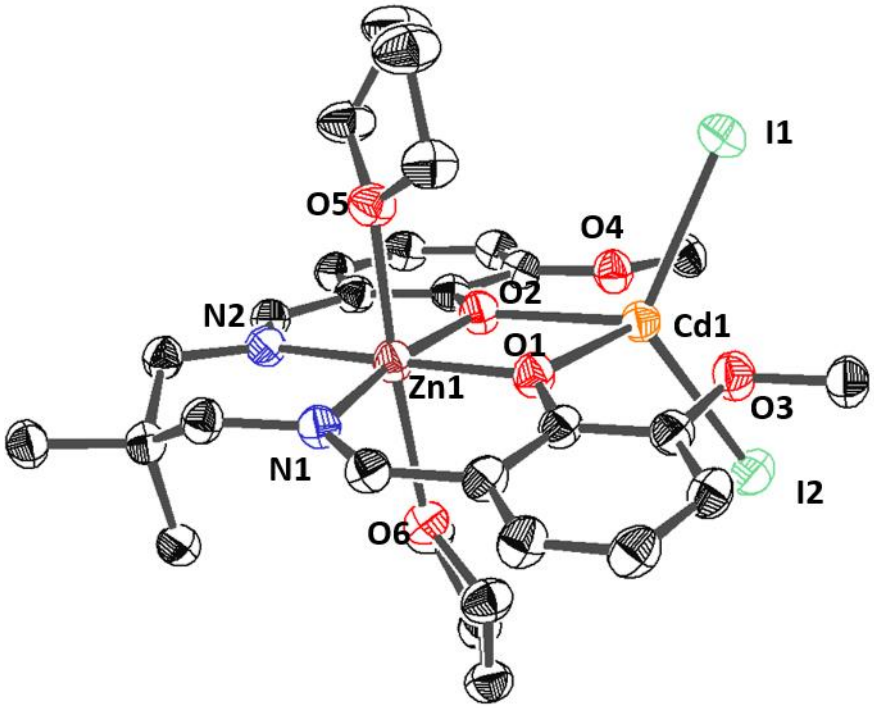

Figure S21: ORTEP representation of the molecular structure of (**6**), with disorder and hydrogen atoms omitted for clarity and thermal ellipsoids represented at 40 % probability.

Table S6: Selected bond lengths (Å) and angles (°) for complex (**6**).

Bond	**Bond Length (Å)**	**Bond**	**Bond Angle (°)**
N (1) – Zn (1)	2.061(4)	N (1) – Zn (1) – O (2)	170.93(15)
N (2) – Zn (1)	2.057(4)	N (2) – Zn (1) – O (1)	172.99(15)
O (1) – Zn (1)	2.032(3)	O (5) – Zn (1) – O (6)	175.73(14)
O (2) – Zn (1)	2.019(3)	O (1) – Cd (1) – O (4)	134.64(11)
O (5) – Zn (1)	2.416(4)	O (1) – Cd (1) – I (2)	111.84(9)
O (6) – Zn (1)	2.191(4)	I (1) – Ca (1) – I (2)	122.381(15)
O (1) – Cd (1)	2.304(3)	**Metal – Metal**	**Distance (Å)**
O (2) – Cd (1)	2.277(3)		
I (1) – Cd (1)	2.7346(4)	Zn (1) – Cd (1)	3.4020(8)
I (2) – Cd (1)	3.7571(5)		

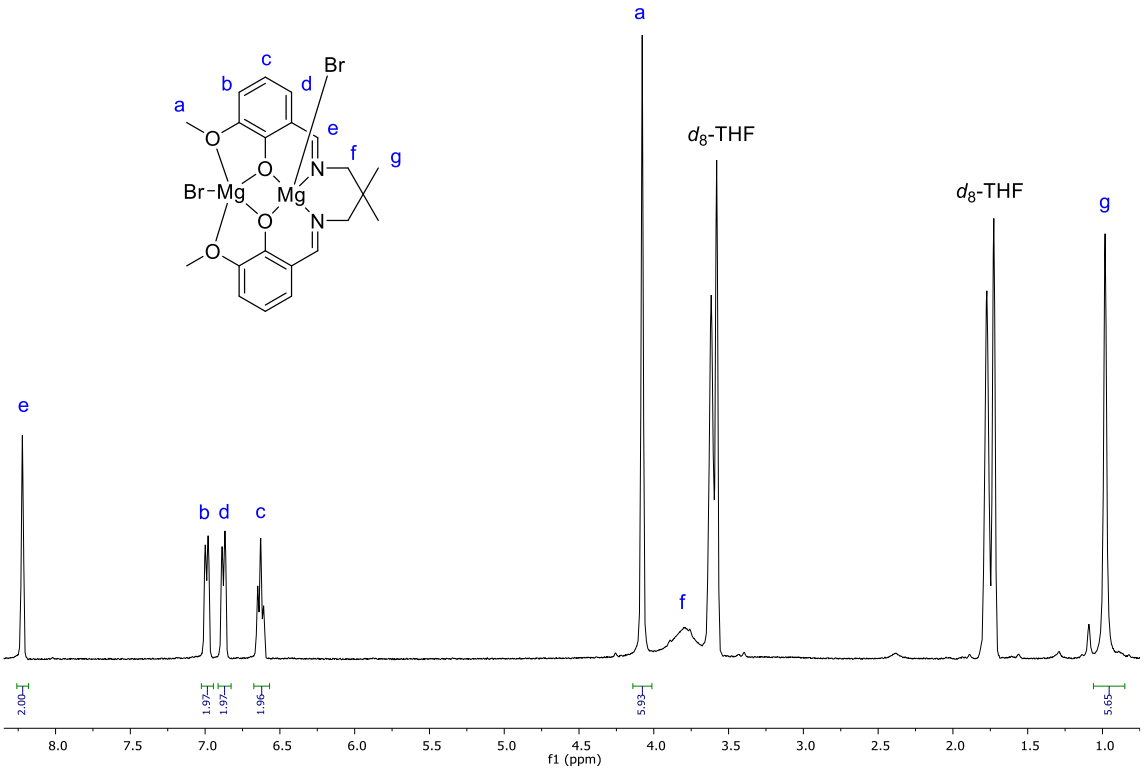

Figure S22: ^{1}H NMR spectrum of (**7**) (d_8-THF, 298 K).

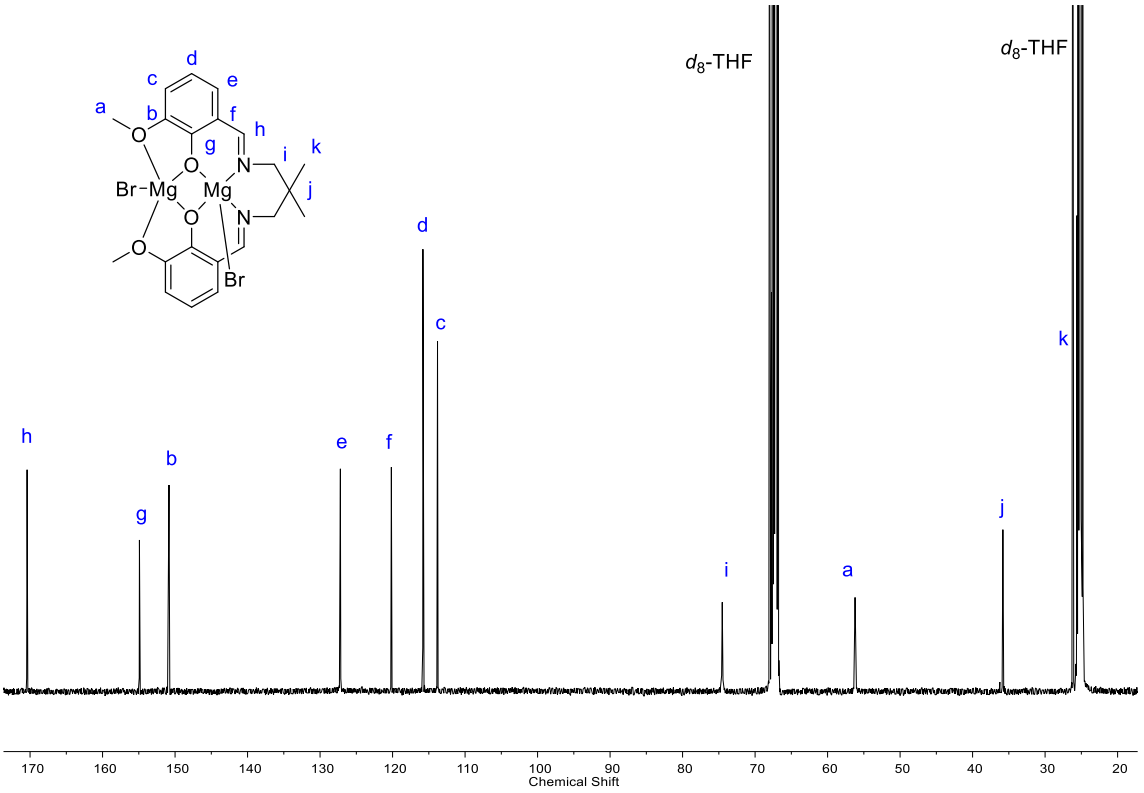

Figure S23: ^{13}C{^{1}H} NMR spectrum of (**7**) (d_8-THF, 298 K).

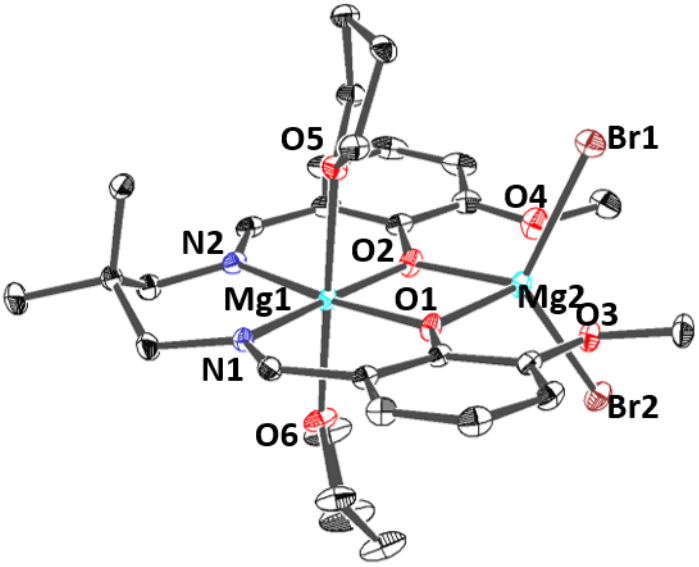

Figure S24: Connectivity molecular structure of (**7**), with disorder and hydrogen atoms omitted for clarity and thermal ellipsoids represented at 40 % probability.

Table S7: Selected bond lengths (Å) and angles (°) for complex (**7**).

Bond	**Bond Length (Å)**	**Bond**	**Bond Angle (°)**
N (1) – Mg (1)	2.100(3)	N (1) – Mg (1) – O (2)	171.60(12)
N (2) – Mg (1)	2.092(3)	N (2) – Mg (1) – O (1)	171.98(12)
O (1) – Mg (1)	1.971(3)	O (5) – Mg (1) – O (1)	89.02(11)
O (2) – Mg (1)	1.969(3)	O (1) – Mg (2) – O (2)	77.06(10)
O (5) – Mg (1)	2.182(3)	O (1) – Mg (2) – Br (2)	109.43(9)
O (6) – Mg (1)	2.163(3)	Br (1) – Mg (2) – Br (2)	124.79(5)
O (1) – Mg (2)	2.057(3)	**Metal – Metal**	**Distance (Å)**
O (2) – Mg (2)	2.042(3)		
O (3) – Mg (2)	2.499(3)	Mg (1) – Mg (2)	**3.103(15)**
O (4) – Mg (2)	2.499(3)		
Br (1) – Mg (2)	2.517(12)		
Br (2) – Mg (2)	2.504(13)		

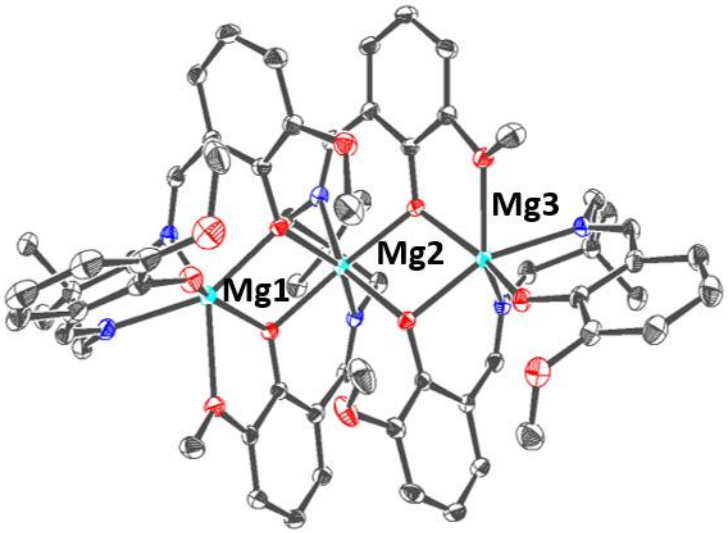

Figure S25: Connectivity structure of the molecular structure of (**8**), with disorder and hydrogen atoms omitted for clarity and thermal ellipsoids represented at 40 % probabiliy.

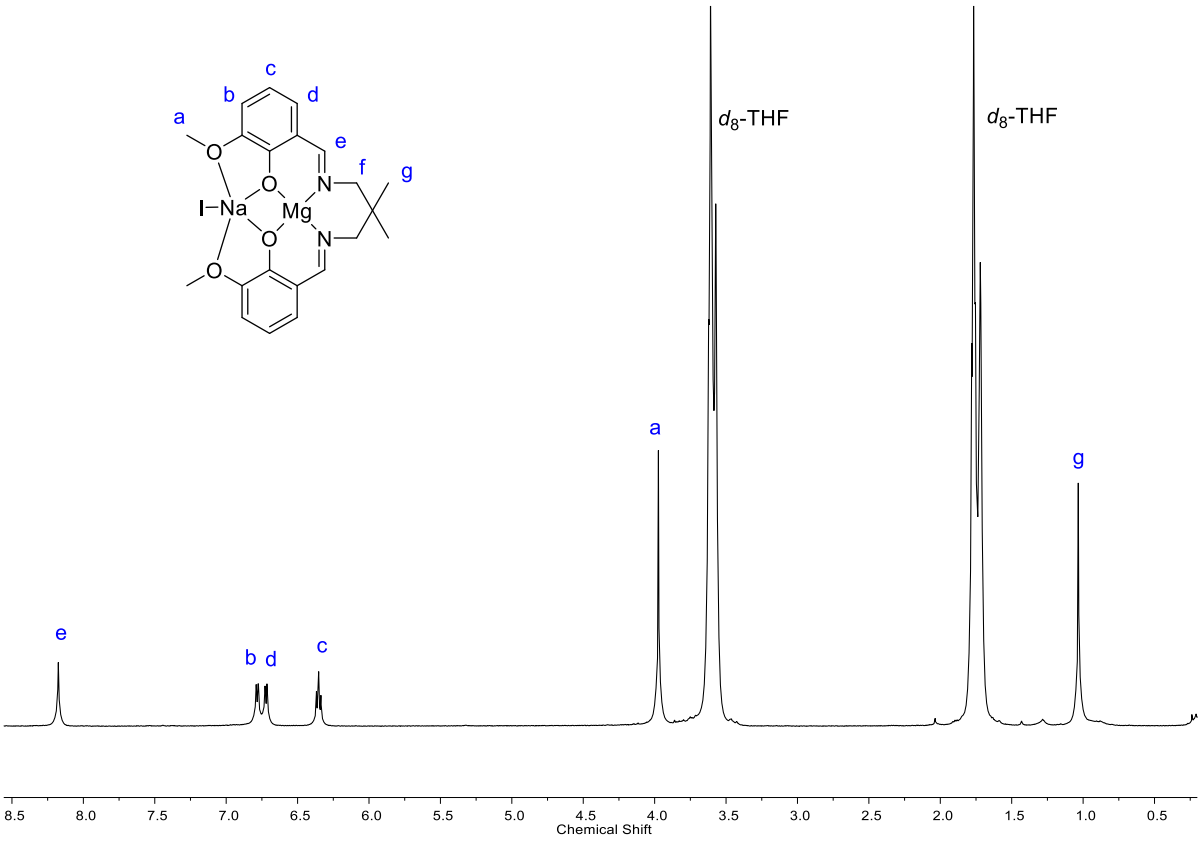

Figure S26: ^{1}H NMR spectrum of (**9**) (d_8-THF, 298 K).

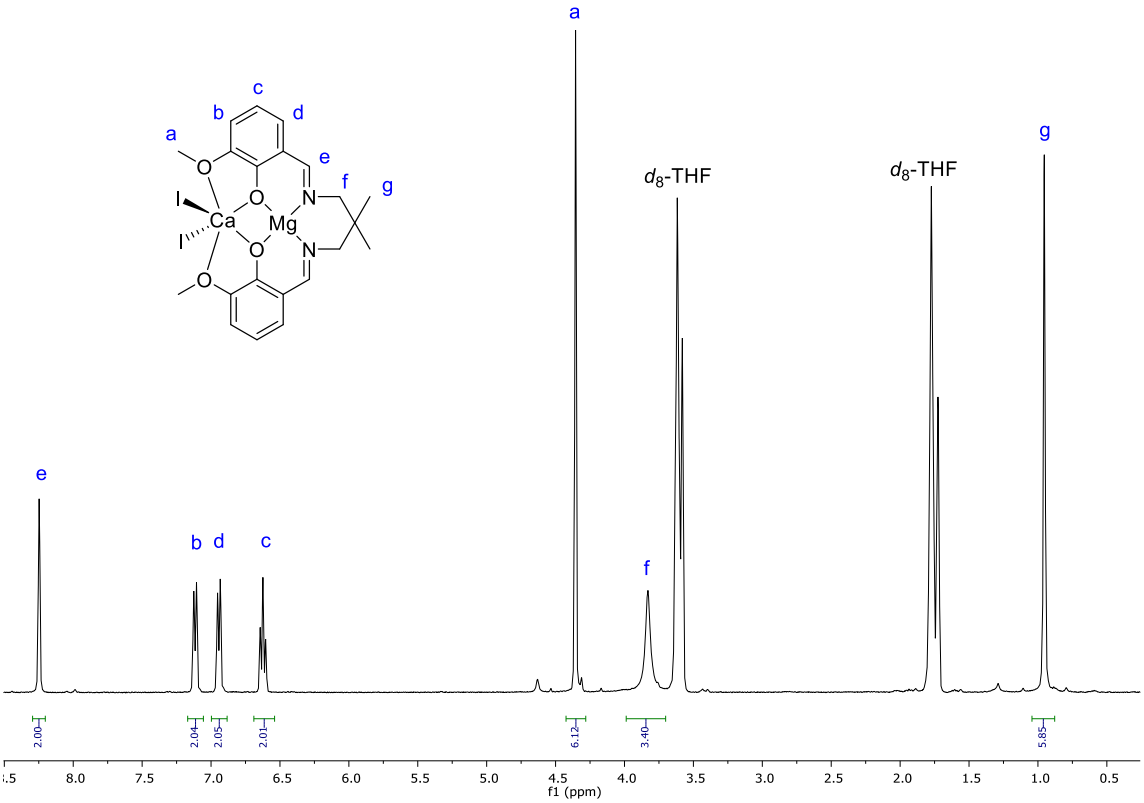

Figure S27: ^{1}H NMR spectrum of (**10**) (d_8-THF, 298 K).

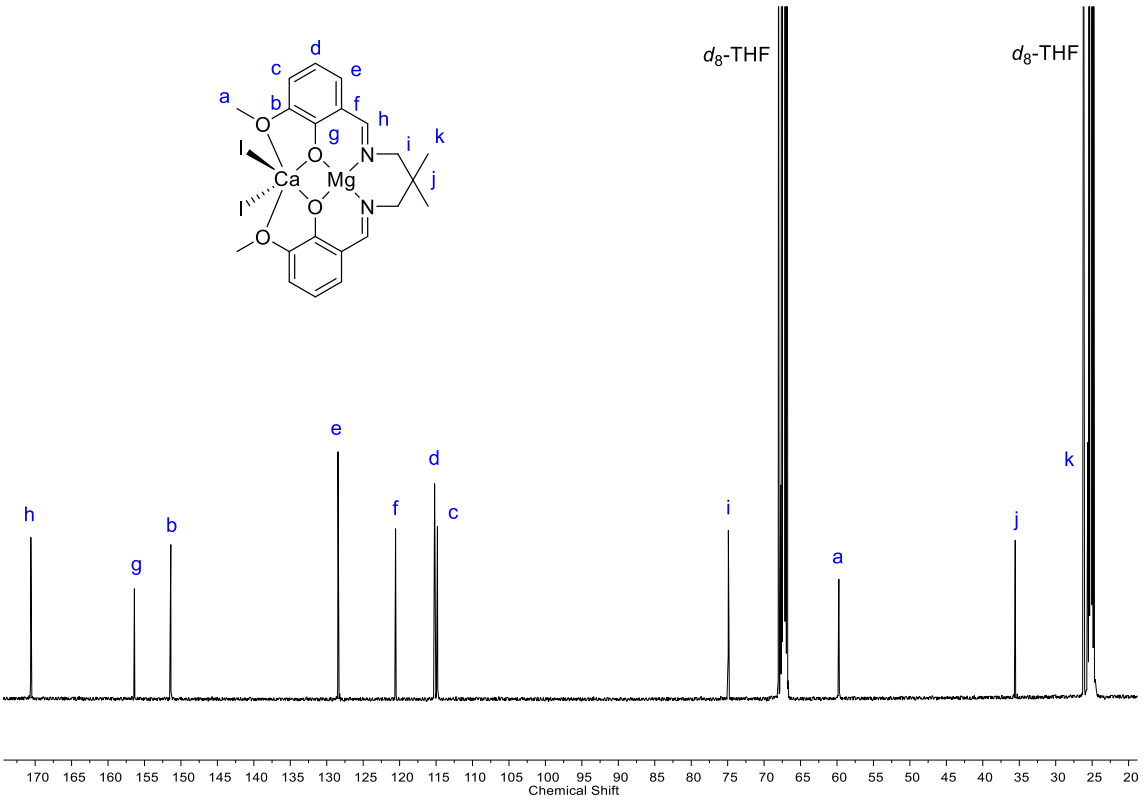

Figure S28: ^{13}C{^{1}H} NMR of (**10**) (d_8-THF, 298 K).

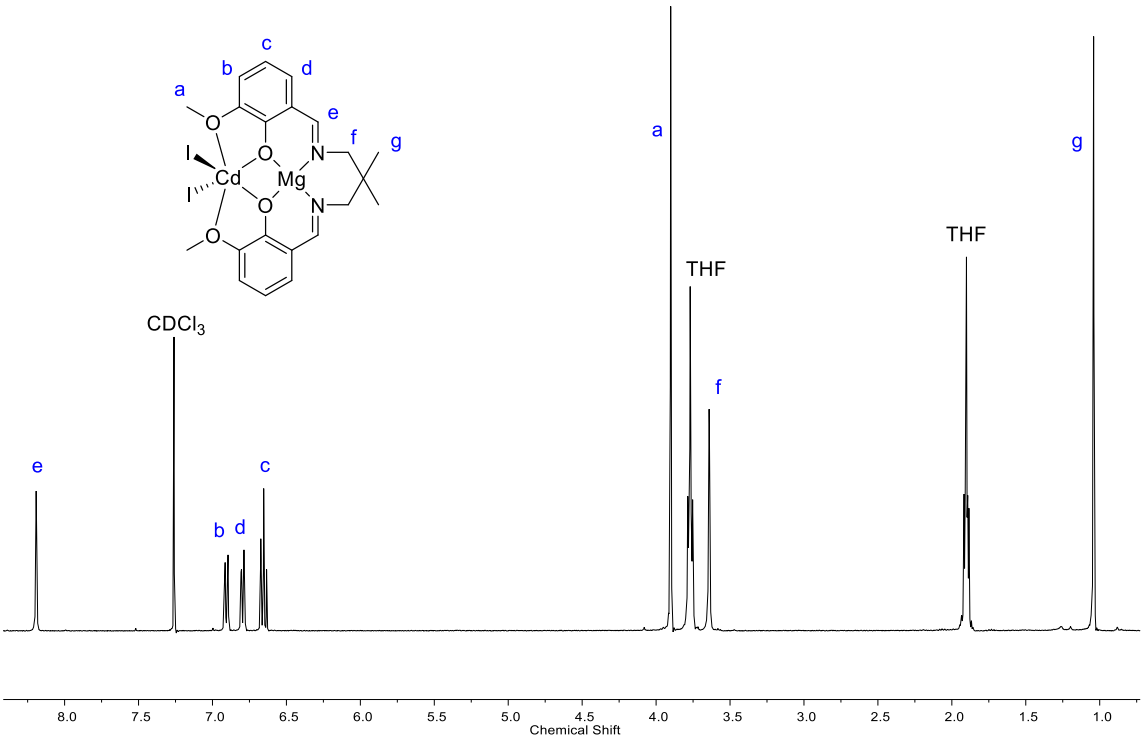

Figure S29: ^{1}H NMR spectrum of (**11**) ($CDCl_3$, 298 K).

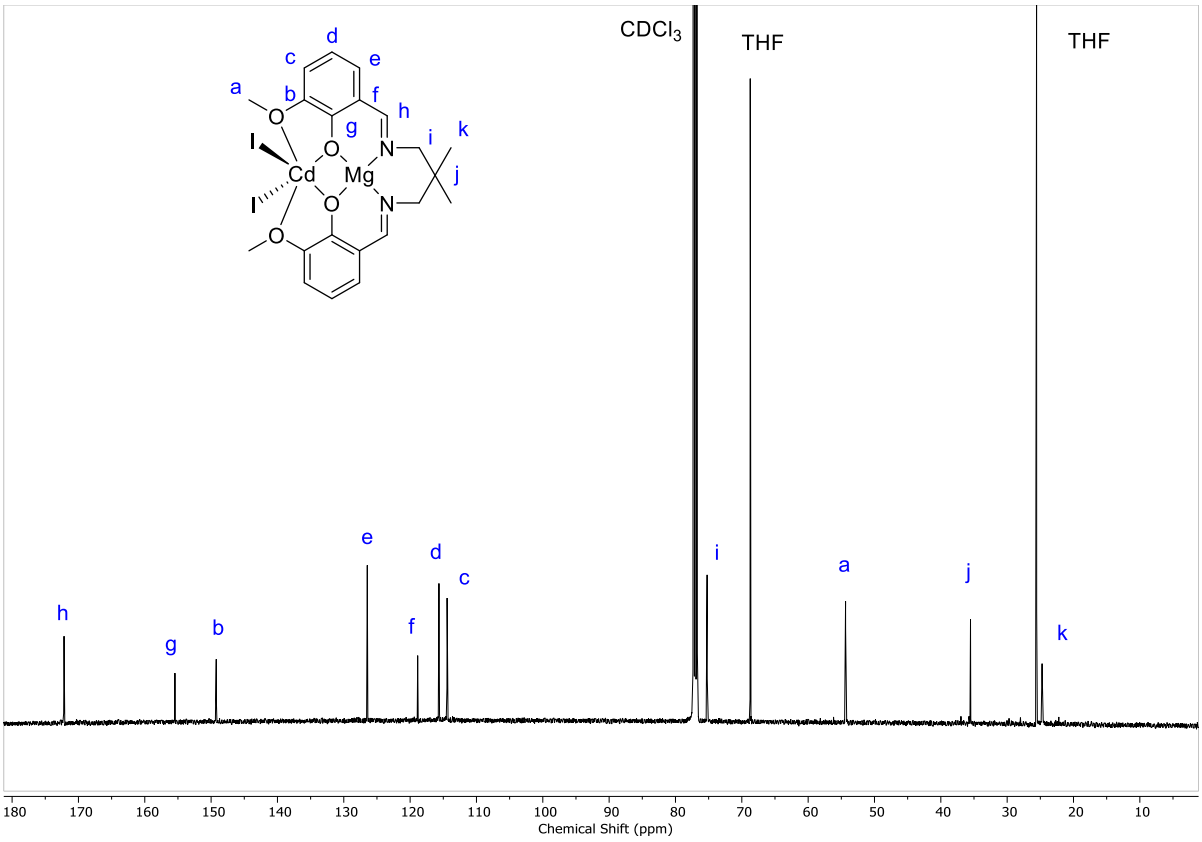

Figure S30: $^{13}C\{^{1}H\}$ NMR spectrum of (**11**) ($CDCl_3$, 298 K).

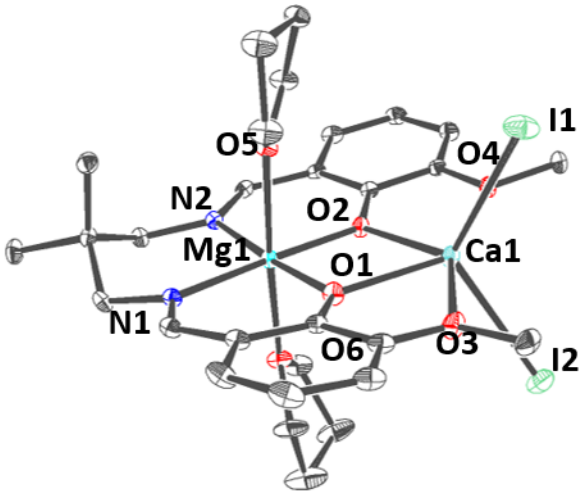

Figure S31: ORTEP representation of the molecular structure of (**10**), with disorder and hydrogen atoms omitted for clarity and thermal ellipsoids represented at 40 % probability.

Table S8: Selected bond lengths (Å) and angles (°) for complex (**10**).

Bond	**Bond Length (Å)**	**Bond**	**Bond Angle (°)**
N (1) – Mg (1)	2.125(3)	N (1) – Mg (1) – O (2)	173.82(11)
N (2) – Mg (1)	2.104(3)	N (2) – Mg (1) – O (1)	175.09(10)
O (1) – Mg (1)	1.976(2)	O (5) – Mg (1) – O (1)	176.48(10)
O (2) – Mg (1)	1.968(2)	O (1) – Ca (1) – O (2)	134.26(8)
O (5) – Mg (1)	2.247(2)	O (1) – Ca (1) – I (2)	111.44(6)
O (6) – Mg (1)	2.133(3)	I (1) – Ca (1) – I (2)	120.73(2)
O (1) – Ca (1)	2.317(2)	**Metal – Metal**	**Distance (Å)**
O (2) – Ca (1)	2.296(2)		
O (3) – Ca (1)	2.527(2)	Mg (1) – Ca (1)	3.3470(11)
O (4) – Ca (1)	2.499(2)		
I (1) – Ca (1)	2.9770(7)		
I (2) – Ca (1)	2.9490(7)		

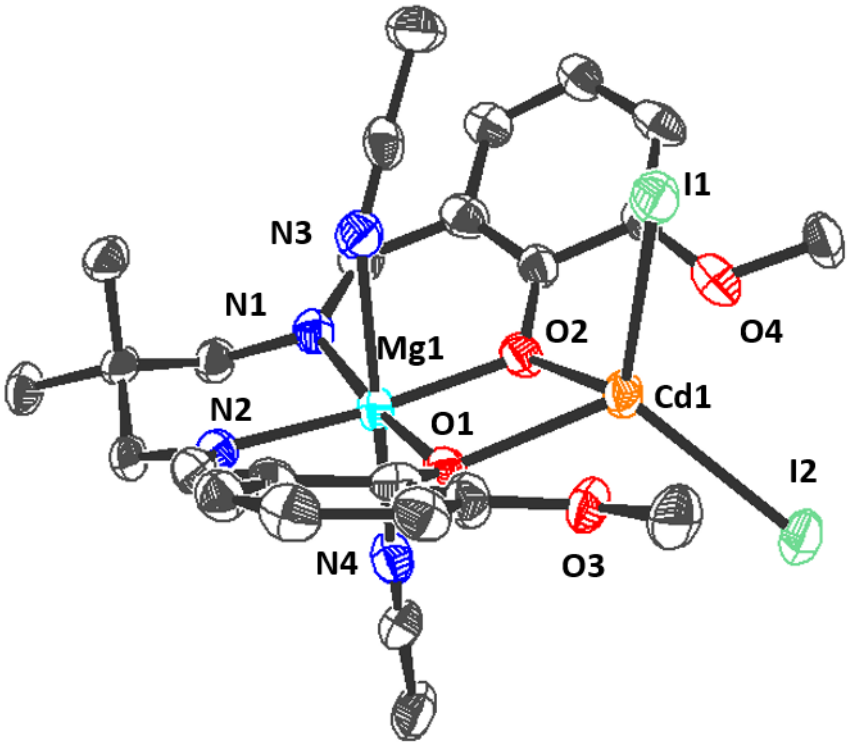

Figure S32: ORTEP representation of the molecular structure of (**11**), with disorder and hydrogen atoms omitted for clarity and thermal ellipsoids represented at 40 % probability.

Table S9: Selected bond lengths (Å) and angles (°) for complex (**11**).

Bond	**Bond Length (Å)**	**Bond**	**Bond Angle (°)**
N (1) – Mg (1)	2.107(8)	N (1) – Mg (1) – O (2)	91.5(3)
N (2) – Mg (1)	2.122(8)	N (2) – Mg (1) – O (1)	94.8(3)
O (1) – Mg (1)	1.971(7)	N (3) – Mg (1) – O (1)	88.4(3)
O (2) – Mg (1)	1.986(7)	O (1) – Cd (1) – O (2)	72.3(2)
N (3) – Mg (1)	2.222(10)	O (1) – Cd (1) – I (2)	84.9(14)
N (4) – Mg (1)	2.361(9)	I (1) – Cd (1) – I (2)	117.8(3)
O (1) – Cd (1)	2.307(6)	**Metal – Metal**	**Distance (Å)**
O (2) – Cd (1)	2.305(6)		
O (3) – Cd (1)	2.623(7)	Mg (1) – Cd (1)	**3.290(3)**
O (4) – Cd (1)	2.606(7)		
I (1) – Cd (1)	2.762(9)		
I (2) – Cd (1)	2.737(9)		

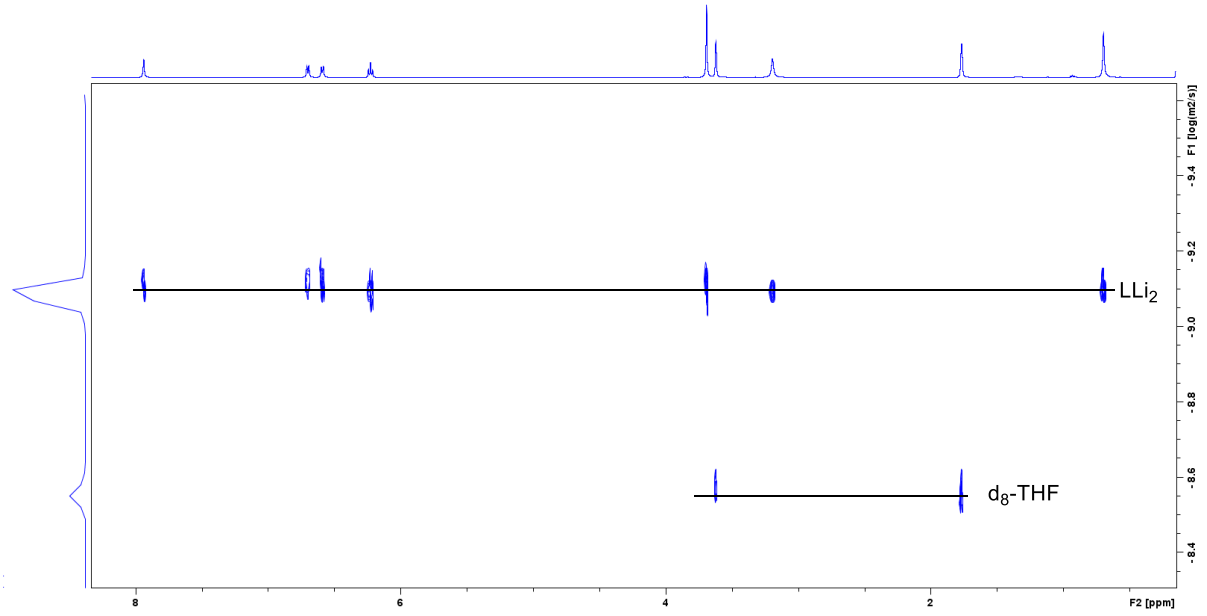

Figure S33: DOSY NMR spectrum of (**1**) in (d_8-THF, 298 K).

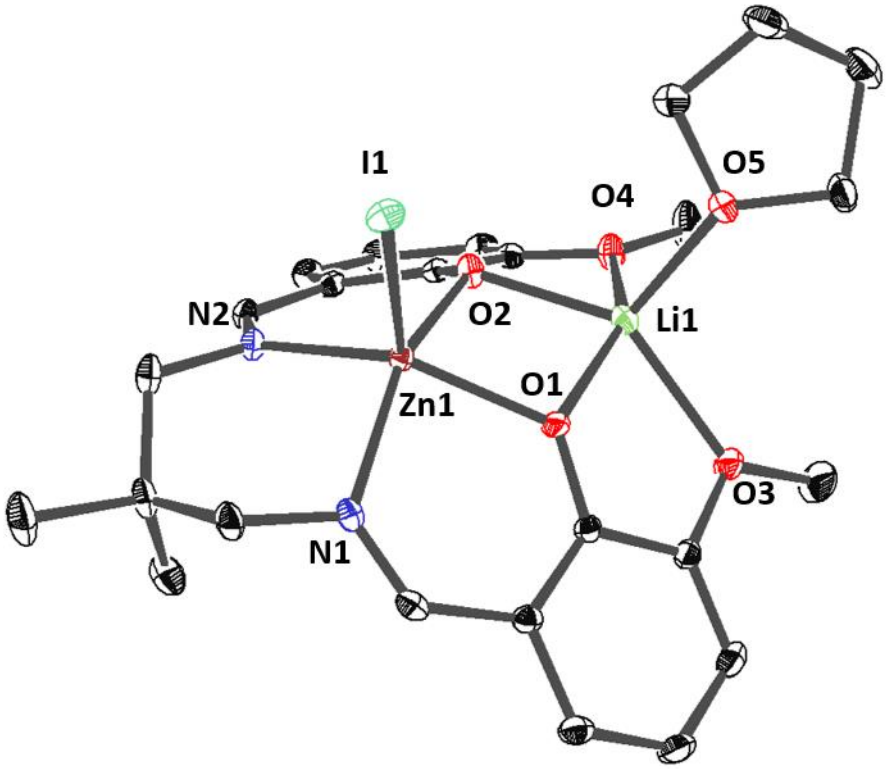

.

Figure S34: ORTEP representation of the molecular structure of (**A**) with disorder and hydrogen atoms omitted for clarity with thermal ellipsoids represented at 40 % probability.

Table S10: Selected bond lengths (Å) and angles (°) for complex (**A**).

Bond	**Bond Length (Å)**	**Bond**	**Bond Angel (°)**
N (1) – Zn (1)	2.0990(17)	N (1) – Zn (1) – O (2)	150.09(7)
N (2) – Zn (1)	2.0862(17)	N (2) – Zn (1) – O (1)	141.82(7)
O (1) – Zn (1)	2.0165(15)	N (1) – Zn (1) – I (1)	101.66(5)
O (2) – Zn (1)	2.0389(14)	O (1) – Li (1) – O (5)	119.8(2)
I (1) – Zn (1)	2.6219(3)	O (2) – Li (1) – O (3)	142.89(19)
O (1) – Li (1)	1.933(4)	O (1) – Li (1) – O (4)	143.5(2)
O (2) – Li (1)	1.994(4)		
O (3) – Li (1)	2.196(4)	**Metal – Metal**	**Distance (Å)**
O (4) – Li (1)	2.143(4)		
O (5) – Li (1)	1.935(4)	Zn (1) – Li (1)	3.070(4)

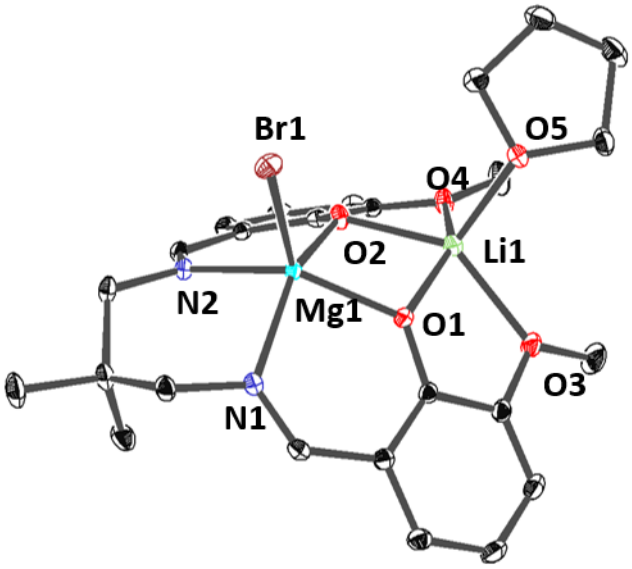

Figure S35: ORTEP representation of the molecular structure of (**B**) with disorder and hydrogen atoms (excluding NH) omitted for clarity with thermal ellipsoids represented at 40 % probability.

Table S11: Selected bond lengths (Å) and angles (°) for complex (**B**).

Bond	**Bond Length (Å)**	**Bond**	**Bond Angle (°)**
N (1) – Mg (1)	2.1443(11)	N (1) – Mg (1) – O (2)	147.41(5)
N (2) – Mg (1)	2.1450(12)	N (2) – Mg (1) – O (1)	143.07(5)
O (1) – Mg (1)	1.9720(10)	Br (1) – Mg (1) – O (1)	101.44(3)
O (2) – Mg (1)	1.9740(10)	O (1) – Li (1) – O (4)	145.45(13)
Br (1) – Mg (1)	2.5091(4)	O (2) – Li (1) – O (3)	141.56(12)
O (1) – Li (1)	1.971(2)	O (1) – Li (1) – O (5)	117.93(13)
O (2) – Li (1)	1.999(3)	**Metal – Metal**	**Distance (Å)**
O (3) – Li (1)	2.148(3)		
O (4) – Li (1)	2.170(3)	Zn (1) – Li (1)	3.001(2)
O (5) – Li (1)	1.947(2)		

Complex	**1**	**2**	**3**	**4**
Local Code	051ckw17	070ckw17	049ckw17	063ckw17
Chemical formula	$C_{42}H_{48}Li_4N_4O_8$	$C_{25}H_{32}I_2N_2O_5Zn_2 \cdot 2(C_4H_8O)$	$C_{42}H_{48}N_4O_8Zn_2$	$C_{33}H_{48}IN_2NaO_7Zn$
M_r	764.60	969.26	867.58	799.99
Crystal system, space group	Tetragonal, $P4_12_12$	Monoclinic, $P2_1$	Monoclinic, $P2_1/c$	Monoclinic, $P2_1/c$
Temperature (K)	150	150	150	150
a, *b*, *c* (Å)	11.2287 (4), 11.2287 (4), 32.691 (2)	10.3649 (2), 17.3850 (4), 10.4787 (2)	10.7086 (1), 20.5174 (2), 8.9876 (1)	21.0024 (5), 10.5844 (2), 15.9024 (3)
α, β, γ (°)	90, 90, 90	90, 93.802 (2), 90	90, 98.462 (1), 90	90, 91.002 (2), 90
V (Å³)	4121.8 (4)	1884.04 (7)	1953.19 (3)	3534.53 (13)
Z	4	2	2	4
Radiation type	Cu *K*α	Cu *K*α	Cu *K*α	Cu *K*α
μ (mm^{-1})	0.68	14.80	2.00	8.33
Crystal size (mm)	0.2 × 0.2 × 0.1	0.25 × 0.08 × 0.05	0.25 × 0.25 × 0.15	0.25 × 0.25 × 0.15
Diffractometer	SuperNova, Dual, Cu at zero, Atlas	SuperNova, Dual, Cu at zero, Atlas	SuperNova, Dual, Cu at zero, Atlas	SuperNova, Dual, Cu at zero, Atlas
Absorption correction	Multi-scan *CrysAlis PRO* 1.171.38.43b (Rigaku Oxford Diffraction, 2015) Empirical absorption correction using spherical harmonics, implemented in SCALE3 ABSPACK scaling algorithm.	Multi-scan *CrysAlis PRO* 1.171.38.43b (Rigaku Oxford Diffraction, 2015) Empirical absorption correction using spherical harmonics, implemented in SCALE3 ABSPACK scaling algorithm.	Multi-scan *CrysAlis PRO* 1.171.38.43b (Rigaku Oxford Diffraction, 2015) Empirical absorption correction using spherical harmonics, implemented in SCALE3 ABSPACK scaling algorithm.	Multi-scan *CrysAlis PRO* 1.171.38.43b (Rigaku Oxford Diffraction, 2015) Empirical absorption correction using spherical harmonics, implemented in SCALE3 ABSPACK scaling algorithm.
T_{min}, T_{max}	0.943, 1	0.308, 1	0.655, 1	0.471, 1
No. of measured, independent and observed [$I > 2\sigma(I)$] reflections	18274, 4279, 3536	15964, 6252, 5971	21024, 4067, 3827	22541, 7305, 6167
R_{int}	0.036	0.049	0.031	0.038
$(\sin \theta/\lambda)_{max}$ ($Å^{-1}$)	0.630	0.629	0.630	0.629
$R[F^2 > 2\sigma(F^2)]$, $wR(F^2)$, S	0.049, 0.126, 1.06	0.042, 0.113, 1.03	0.031, 0.084, 1.02	0.038, 0.102, 1.04
No. of reflections	4279	6252	4067	7305
No. of parameters	266	465	257	421
No. of restraints	0	131	0	48
H-atom treatment	H-atom parameters constrained	H-atom parameters constrained	H-atom parameters constrained	H-atom parameters constrained
	$w = 1/[\sigma^2(F_o^2) + (0.0439P)^2 + 1.5085P]$ where $P = (F_o^2 + 2F_c^2)/3$	$w = 1/[\sigma^2(F_o^2) + (0.0787P)^2 + 0.565P]$ where $P = (F_o^2 + 2F_c^2)/3$	$w = 1/[\sigma^2(F_o^2) + (0.0508P)^2 + 1.0504P]$ where $P = (F_o^2 + 2F_c^2)/3$	$w = 1/[\sigma^2(F_o^2) + (0.057P)^2 + 1.9705P]$ where $P = (F_o^2 + 2F_c^2)/3$
$\Delta\rho_{max}$, $\Delta\rho_{min}$ (e $Å^{-3}$)	0.16, −0.15	1.17, −0.89	0.31, −0.34	0.77, −0.61
Absolute structure	Flack x determined using 1171 quotients [(I+)-(I-)]/[(I+)+(I-)] (Parsons, Flack and Wagner, Acta Cryst. B69 (2013) 249-259).	Refined as an inversion twin.	–	–
Absolute structure parameter	0.03 (12)	0.420 (7)	–	–

Complex	**5**	**6**	**7**	**8**
Local Code	009CKW17	075ckw17	012rwfk20	045ckw17
Chemical formula	$C_{29}H_{40}CaI_2N_2O_6Zn$ ·C_4H_8O	$C_{29}H_{40}CdI_2N_2O_6Zn$	$C_{29}H_{40}Br_2Mg_2N_2O_6$ ·2(C_4H_8O)	$C_{63}H_{72}Mg_3N_6O_{12}$
M_r	943.98	944.20	865.27	1178.19
Crystal system, space group	Orthorhombic, *Pbca*	Triclinic, *P*1	Monoclinic, $P2_1/n$	Orthorhombic, $Pna2_1$
Temperature (K)	150	150	150	150
a, *b*, *c* (Å)	13.9060 (2), 14.3422 (2), 37.8508 (5)	10.1985 (2), 10.9552 (3), 15.6105 (3)	10.7118 (2), 20.0019 (2), 18.6537 (3)	26.6385 (5), 12.1506 (2), 18.5863 (3)
α, β, γ (°)	90, 90, 90	86.416 (2), 87.592 (2), 73.094 (2)	90, 91.671 (1), 90	90, 90, 90
V (Å^3)	7549.06 (18)	1664.95 (7)	3994.97 (11)	6015.90 (18)
Z	8	2	4	4
Radiation type	Cu *K*α	Cu *K*α	Cu *K*α	Cu *K*α
μ (mm^{-1})	15.31	20.90	3.30	1.01
Crystal size (mm)	0.25 × 0.25 × 0.04	0.2 × 0.1 × 0.05 × 0.1 (radius)	0.20 × 0.08 × 0.07	0.2 × 0.2 × 0.01
Diffractometer	SuperNova, Dual, Cu at zero, Atlas	SuperNova, Dual, Cu at zero, Atlas	SuperNova, Dual, Cu at home/near, Atlas	SuperNova, Dual, Cu at zero, Atlas
Absorption correction	Multi-scan *CrysAlis PRO* 1.171.38.43b (Rigaku Oxford Diffraction, 2015) Empirical absorption correction using spherical harmonics, implemented in SCALE3 ABSPACK scaling algorithm.	For a sphere *CrysAlis PRO* 1.171.38.43b (Rigaku Oxford Diffraction, 2015) Spherical absorption correction using equivalent radius and absorption coefficient. Empirical absorption correction using spherical harmonics, implemented in SCALE3 ABSPACK scaling algorithm.	Multi-scan *CrysAlis PRO* 1.171.41.81a (Rigaku Oxford Diffraction, 2020) Empirical absorption correction using spherical harmonics, implemented in SCALE3 ABSPACK scaling algorithm.	Multi-scan *CrysAlis PRO* 1.171.38.43b (Rigaku Oxford Diffraction, 2015) Empirical absorption correction using spherical harmonics, implemented in SCALE3 ABSPACK scaling algorithm.
T_{min}, T_{max}	0.095, 1	0.002, 0.041	0.684, 1.000	0.707, 1
No. of measured, independent and observed [$I > 2\sigma(I)$] reflections	28061, 7815, 6911	36207, 6905, 6596	35779, 8364, 6656	38599, 10130, 9223
R_{int}	0.046	0.045	0.042	0.061
(sin θ/λ)$_{max}$ (Å^{-1})	0.630	0.630	0.631	0.630
$R[F^2 > 2\sigma(F^2)]$, $wR(F^2)$, S	0.035, 0.094, 1.06	0.082, 0.180, 1.22	0.052, 0.153, 1.08	0.046, 0.123, 1.01
No. of reflections	7815	6905	8364	10130
No. of parameters	512	370	464	767
No. of restraints	165	0	0	2
H-atom treatment	H-atom parameters constrained	H-atom parameters constrained	H-atom parameters constrained	H-atom parameters constrained
	$w = 1/[\sigma^2(F_o^2) + (0.0484P)^2 + 3.3617P]$ where $P = (F_o^2 + 2F_c^2)/3$	$w = 1/[\sigma^2(F_o^2) + (0.1354P)^2]$ where $P = (F_o^2 + 2F_c^2)/3$	$w = 1/[\sigma^2(F_o^2) + (0.0692P)^2 + 6.8338P]$ where $P = (F_o^2 + 2F_c^2)/3$	$w = 1/[\sigma^2(F_o^2) + (0.0695P)^2 + 1.7386P]$ where $P = (F_o^2 + 2F_c^2)/3$
$\Delta\rho_{max}$, $\Delta\rho_{min}$ (e Å^{-3})	1.61, −0.93	3.49, −0.64	1.59, −0.46	0.77, −0.31
Absolute structure	–	–	–	Flack x determined using 2985 quotients [(I+)-(I-)]/[(I+)+(I-)] (Parsons, Flack and Wagner, Acta Cryst. B69 (2013) 249-259).
Absolute structure parameter	–	–	–	0.11 (4)

Complex	**10**	**11**	**A**	**B**
Local Code	005ckw17	011rwfk20	033ckw17	044ckw17
Chemical formula	$C_{29}H_{40}CaI_2MgN_2O_6$	$C_{25}H_{30}CdI_2MgN_4O_4$	$C_{25}H_{32}ILiN_2O_5Zn$	$C_{25}H_{32}BrLiMgN_2O_5$
M_r	830.82	841.04	639.73	551.68
Crystal system, space group	Triclinic, *P*1	Monoclinic, $P2_1/c$	Monoclinic, $P2_1/c$	Monoclinic, $P2_1/c$
Temperature (K)	150	150	150	150
a, *b*, *c* (Å)	10.3461 (3), 10.9492 (3), 15.5339 (4)	10.7707 (3), 17.2439 (7), 19.6341 (6)	12.2484 (3), 11.1331 (3), 19.8508 (5)	12.3544 (1), 10.9625 (1), 19.5187 (1)
α, β, γ (°)	85.232 (2), 88.170 (2), 73.452 (2)	90, 90.981 (3), 90	90, 91.174 (2), 90	90, 90.048 (1), 90
V (Å^3)	1680.92 (8)	3646.1 (2)	2706.34 (12)	2643.52 (3)
Z	2	4	4	4
Radiation type	Cu *K*α	Mo *K*α	Cu *K*α	Cu *K*α
μ (mm^{-1})	16.55	2.34	10.51	2.66
Crystal size (mm)	0.25 × 0.08 × 0.04	0.25 × 0.14 × 0.09	0.25 × 0.18 × 0.06	0.15 × 0.1 × 0.05
Diffractometer	SuperNova, Dual, Cu at zero, Atlas	SuperNova, Dual, Cu at home/near, Atlas	SuperNova, Dual, Cu at zero, Atlas	SuperNova, Dual, Cu at zero, Atlas
Absorption correction	Multi-scan *CrysAlis PRO* 1.171.38.43b (Rigaku Oxford Diffraction, 2015) Empirical absorption correction using spherical harmonics, implemented in SCALE3 ABSPACK scaling algorithm.	Multi-scan *CrysAlis PRO* 1.171.39.46e (Rigaku Oxford Diffraction, 2018) Empirical absorption correction using spherical harmonics, implemented in SCALE3 ABSPACK scaling algorithm.	Multi-scan *CrysAlis PRO* 1.171.38.43b (Rigaku Oxford Diffraction, 2015) Empirical absorption correction using spherical harmonics, implemented in SCALE3 ABSPACK scaling algorithm.	Multi-scan *CrysAlis PRO* 1.171.38.43b (Rigaku Oxford Diffraction, 2015) Empirical absorption correction using spherical harmonics, implemented in SCALE3 ABSPACK scaling algorithm.
T_{min}, T_{max}	0.146, 1	0.816, 1.000	0.294, 1	0.876, 1
No. of measured, independent and observed [$I > 2\sigma(I)$] reflections	35018, 6958, 6420	31683, 9479, 6441	15838, 5603, 5160	62976, 5531, 5261
R_{int}	0.049	0.066	0.027	0.043
$(\sin\theta/\lambda)_{max}$ (Å^{-1})	0.630	0.698	0.630	0.630
$R[F^2 > 2\sigma(F^2)]$, $wR(F^2)$, *S*	0.036, 0.107, 1.03	0.082, 0.287, 1.04	0.022, 0.055, 1.02	0.025, 0.069, 1.06
No. of reflections	6958	9479	5603	5531
No. of parameters	370	340	320	320
No. of restraints	0	0	0	0
H-atom treatment	H-atom parameters constrained	H-atom parameters constrained	H-atom parameters constrained	H-atom parameters constrained
	$w = 1/[\sigma^2(F_o^2) + (0.0684P)^2 + 1.777P]$ where $P = (F_o^2 + 2F_c^2)/3$	$w = 1/[\sigma^2(F_o^2) + (0.1775P)^2 + 18.5985P]$ where $P = (F_o^2 + 2F_c^2)/3$	$w = 1/[\sigma^2(F_o^2) + (0.0249P)^2 + 1.012P]$ where $P = (F_o^2 + 2F_c^2)/3$	$w = 1/[\sigma^2(F_o^2) + (0.0401P)^2 + 1.0182P]$ where $P = (F_o^2 + 2F_c^2)/3$
$\Delta\rho_{max}$, $\Delta\rho_{min}$ (e Å^{-3})	1.10, −1.00	3.13, −1.66	0.60, −0.57	0.28, −0.39
Absolute structure	–	–	–	–
Absolute structure parameter	–	–	–	–

Computer programs: *CrysAlis PRO* 1.171.38.43b (Rigaku OD, 2015), *CrysAlis PRO* 1.171.39.46e (Rigaku OD, 2018), *CrysAlis PRO* 1.171.41.81a (Rigaku OD, 2020), *SHELXT2014* (Sheldrick, 2014), *SHELXT* (Sheldrick, 2015), *SHELXL* (Sheldrick, 2015), Olex2 (Dolomanov *et al.*, 2009).

References

1. G. M. Sheldrick, Acta Cryst. A, 2015, **71**, 3-8
2. G. M Sheldrick, Acta Cryst. C, 2015, **71**, 3-8.
3. O. V. Dolomanov, L. J. Bourhis, R. J. Gildea, J. A. K. Howard and H. Puschmann, J. Appl. Crystallogr., 2009, **42**, 339-341
4. L. J. Farrugia, *J. Appl. Cryst.*, 2012, **45**, 849-854
5. D. J. Darensbourg, R. R. Poland and C. Escobedo, *Macromolecules*, 2012, **45**, 2242-2248
6. J. Y. Jeon, S. C. Eo, J. K. Varghese and B. Y. Lee, *Beilstein J. Org. Chem.*, 2014, **10**, 1787-1795
7. B. A. Abel, C. A. L. Lidston and G. W. Coates, *J. Am. Chem. Soc.*, 2019, **141**, 12760-12769
8. P. K. Saini, C. Romain, Y. Zhu and C. K. Williams, *Polym. Chem.*, 2014, **5**, 6068-6075
9. Z. Shi, Q. Jiang, Z. Song, Z. Wang and C. Gao, *Polym. Chem.*, 2018, **9**, 4733-4743
10. J. Li, Y. Liu, W.-M. Ren and X.-B. Lu, *J. Am. Chem. Soc.*, 2016, **138**, 11493-11496